Quaternary Science Reviews 27 (2008) 1523–1540

Contents lists available at ScienceDirect

Quaternary Science Reviews

journal homepage: www.elsevier.com/locate/quascirev

Palaeoenvironmental dynamics inferred from late Quaternary permafrost deposits on Kurungnakh Island, Lena Delta, Northeast Siberia, Russia

Sebastian Wetterich [a,*], Svetlana Kuzmina [b], Andrei A. Andreev [a], Frank Kienast [c], Hanno Meyer [a], Lutz Schirrmeister [a], Tatyana Kuznetsova [d], Melanie Sierralta [e]

[a] Alfred Wegener Institute for Polar and Marine Research, Research Unit Potsdam, Telegrafenberg A43, D-14473 Potsdam, Germany
[b] Department of Earth and Atmospheric Sciences, University of Alberta, Edmonton, Canada T6G 2E3
[c] Research Institute and Museum for Natural History Senckenberg, Research Station for Quaternary Palaeontology Weimar, Am Jakobskirchhof 4, D-99423 Weimar, Germany
[d] Department of Palaeontology, Moscow State University, Leninskie Gory, 11992 Moscow, Russia
[e] Leibniz Institute for Applied Geosciences, Stilleweg 2, D-30655 Hannover, Germany

ARTICLE INFO

Article history:
Received 12 January 2008
Received in revised form
21 March 2008
Accepted 15 April 2008

ABSTRACT

Late Quaternary palaeoenvironments of the Siberian Arctic were reconstructed by combining data from several fossil bioindicators (pollen, plant macro-fossils, ostracods, insects, and mammal bones) with sedimentological and cryolithological data from permafrost deposits. The record mirrors the environmental history of Beringia and covers glacial/interglacial and stadial/interstadial climate variations with a focus on the Middle Weichselian interstadial (50–32 kyr BP). The late Pleistocene to Holocene sequence on Kurungnakh Island reflects the development of periglacial landscapes under changing sedimentation regimes which were meandering fluvial during the Early Weichselian, colluvial or proluvial on gently inclined plaines during the Middle and Late Weichselian, and thermokarst-affected during the Holocene. Palaeoecological records indicate the existence of tundra–steppe vegetation under cold continental climate conditions during the Middle Weichselian interstadial. Due to sedimentation gaps in the sequence between 32 and 17 kyr BP and 17 and 8 kyr BP, the Late Weichselian stadial is incompletely represented in the studied outcrops. Nevertheless, by several palaeoecological indications arctic tundra–steppe vegetation under extremely cold-arid conditions prevailed during the late Pleistocene. The tundra–steppe disappeared completely due to lasting paludification during the Holocene. Initially subarctic shrub tundra formed, which later retreated in course of the late Holocene cooling.

1. Introduction

The complex composition and structure of late Quaternary ice-rich permafrost deposits in the Siberian Arctic has been investigated by a number of studies in the last decades (e.g. Lungersgauzen, 1961; Tomirdiaro, 1982; Galabala, 1987; Sher et al., 1987; Kunitsky, 1989; Grigoriev, 1993), but the origin of these sediments and their exact stratigraphical classification still remain unclear. Special problems concern the position and characteristic of the so-called Kargin interstadial between 50 and 25 kyr BP according to the regular stratigraphic order in Russia. Despite of legitimate criticism on the stratigraphic position of the stratotyp at Cape Karginsky on the lower Yenissei, which belongs to the Eemian (Kazantsevo) Interglacial (Astakhov, 2001, 2006; Astakhov and Mangerud, 2005) as well as the already revised interglacial environmental interpretation in Northeast Siberia (Kind, 1974) the term Kargin is not substituted yet by the Russian Interdepartmental Stratigraphic Commission on the Quaternary. Therefore, we have to use this term further on as long as no other name is established describing this special late Pleistocene period.

Palaeoenvironmental records from the continental part of the Laptev Sea region link the West Siberian Arctic and Alaska (Fig. 1) and reveal the arctic palaeoenvironments of Beringia—the landmass that connected both regions during the late Pleistocene.

Numerous multidisciplinary publications have already focused on permafrost deposits as late Quaternary palaeoclimate archives in the Siberian Arctic (e.g. Schirrmeister et al., 2002a, b, 2003; Hubberten et al., 2004; Pitulko et al., 2004; Sher et al., 2005; Grosse et al., 2007), especially since other long-term Quaternary records such as lake sediments are rare in this region.

* Corresponding author.
E-mail address: sebastian.wetterich@awi.de (S. Wetterich).

0277-3791/$ - see front matter © 2008 Elsevier Ltd. All rights reserved.
doi:10.1016/j.quascirev.2008.04.007

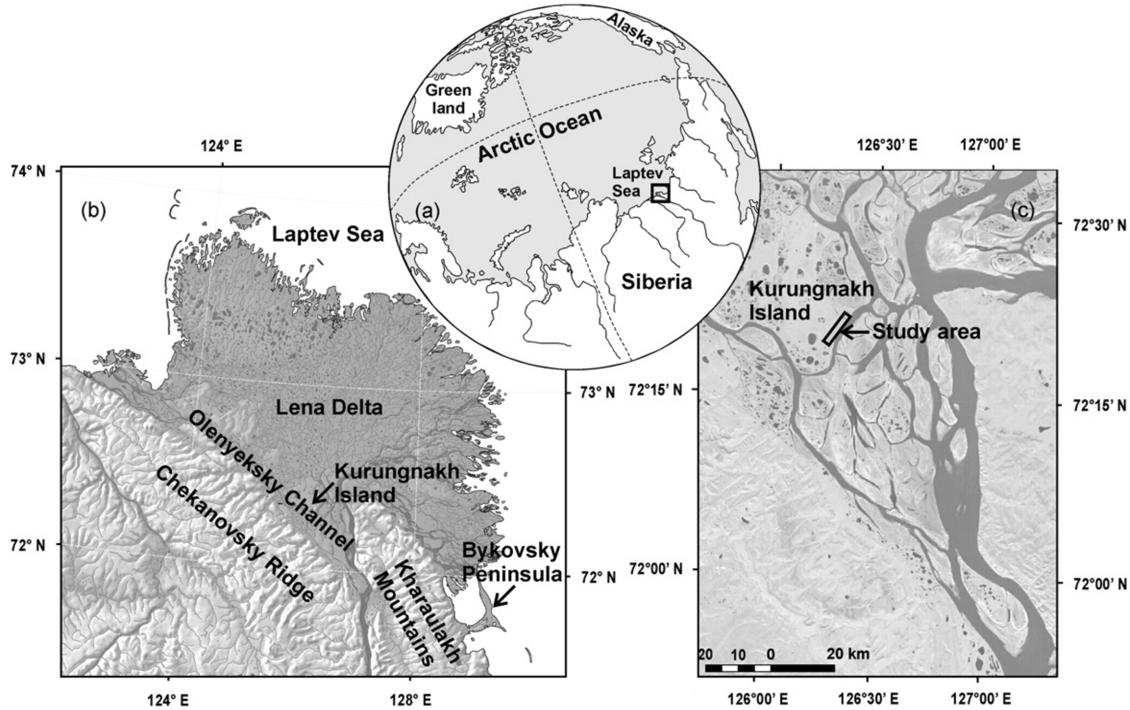

Fig. 1. Position of the study site (a) in Northeast Siberia at the Laptev Sea coast; (b) in the southern part of the Lena Delta; and (c) on Kurungnakh Island.

The generally high content of well-preserved fossil remains in late Quaternary permafrost deposits in combination with sedimentological, geocryological, and stratigraphical descriptions allow detailed reconstructions of environmental and climatic dynamics. Various palaeoproxies in frozen deposits such as pollen (Andreev et al., 2002), plant macro-fossils (Kienast et al., 2005), rhizopods (Bobrov et al., 2004), chironomids (Ilyashuk et al., 2006), freshwater ostracods (Wetterich et al., 2005), insects (Kuzmina and Sher, 2006), and mammal bones (Kuznetsova et al., 2003) as well as stable isotope records of ground ice (Meyer et al., 2002a, b) have been used for reconstructions of late Quaternary palaeoenvironments and palaeoclimate in the Laptev Sea region (Northeast Siberia).

The goal of this study is to describe palaeoecological features and landscape development in the Siberian Arctic in comparison to other palaeorecords from this region. Different regional settings such as the change from an inland to a coastal position due to the late Quaternary marine transgression may alter the information preserved in permafrost deposits.

The study is focused on the Middle Weichselian (Kargin) period, which correlates with the Marine Isotope Stage 3 (MIS-3) when thick ice-rich permafrost deposits (so-called Ice Complex) accumulated. Regional climatic variations within this period are well documented by detailed records of plant macro-fossils and insect remains. Pollen records were interpreted as a supra-regional record.

During three joint Russian–German expeditions in 1998, 2000, and 2002, fieldwork was conducted on outcrops of Kurungnakh Island (Rachold, 1999; Rachold and Grigoriev, 2001; Grigoriev et al., 2003). The results of the expeditions in 1998 and 2000 were summarised by Schwamborn et al. (2002) and Schirrmeister et al. (2003), whereas the results of the work done in 2002 are presented here for the first time. In 2002 we returned to Kurungnakh Island in order to supplement previous studies by sampling the site in more detail and in higher resolution. We aimed to make additional age determinations of the sediments, and receive additional bioindicator data from pollen, plant macro-fossils, freshwater ostracods, insect remains, and mammal bones.

2. Regional setting

The fieldwork was performed in the Lena Delta that is located at the Laptev Sea coast (Fig. 1) in Northeast Siberia. The studied permafrost outcrops were obtained on Kurungnakh Island (72°20′N; 126°18′E) in the southern part of the delta beside the Olenyeksky Channel, which is the major western outlet of the Lena River within the delta.

In this part of the delta several islands remain as fragments of a broad foreland plain north of the Chekanovsky Ridge (Fig. 1). The foreland plain is dissected by several distributaries (outlets) of the lower Lena River and a number of small rivers and brooks that drain the slope of the Chekanovsky Ridge (Schirrmeister et al., 2003).

Kurungnakh Island is mainly composed of late Quaternary sediments that belong to the third Lena River terrace (Grigoriev, 1993) with altitudes up to 40 m above the river level (m a.r.l.). The sediments consist of two main formations (Fig. 2). The first formation is described as sandy deposits that are covered by the second formation that built up by ice-rich peaty and silty Ice Complex deposits (Yedoma Suite). In addition, Holocene deposits are widely distributed on top of the third Lena River terrace in small-scale thermokarst depressions and in fillings of large thermokarst depressions called "alases". Alases are an important landscape-forming feature of the ice-rich permafrost zone, which is mainly caused by extensive melting of ground ice in the underlying permafrost (van Everdingen, 1998). Such sequences of sandy deposits overlain by Ice Complex deposits and frequently interrupted by thermokarst depressions are exposed along the entire Olenyeksky Channel.

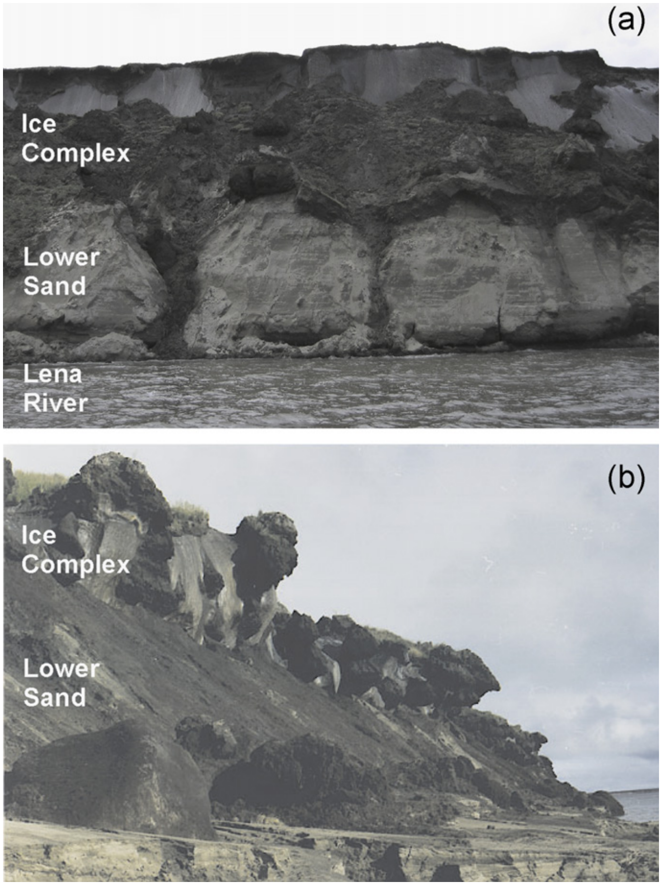

Fig. 2. Exposure situation at Kurungnakh Island: (a) overview of the general stratigraphic configuration along the coast of the Olenyeksky Channel (photograph taken in summer 2000); (b) exposure situation at the sampling sites in 2002.

3. Material and methods

3.1. Sedimentology and cryolithology

Sedimentological and cryolithological features of permafrost deposits from two sections were studied by describing and sampling several subprofiles on coastal exposures of frozen deposits (Fig. 3) in August 2002 by S. Kuzmina and S. Wetterich. The upper section was sampled at 72°20′41″N and 126°18′33″E top down from the island's surface, whereas the lower section was sampled at 72°20′35″N and 126°18′20″E bottom up from the Lena River bank. In total, 53 samples were studied for sedimentological and cryolithological characteristics.

The frozen sediment samples were taken by knife or axe. In the upper part of the section we collected samples along a stratigraphic vertical sequence of thermokarst mounds (baydzherakhs) with overlapping tops and bottoms (Fig. 3). The lower section was sampled at excavations. Various methods were used to characterise the permafrost deposits. While still in the field, the ice content was gravimetrically determined on a dry-weight basis, as the ratio of the mass of ice in a frozen sample to the mass of the dry sample, expressed as a percentage (van Everdingen, 1998). For these purposes we used an electric balance (Kern) for weight determination before and after sample-drying on metal field-oven. Before laboratory analyses all samples were freeze-dried and afterwards prepared for different sedimentological, geochronological, and palaeoecological analyses. The grain-size distribution was measured by Laser Particle Analyser (Beckmann Coulter LS 200). Mass-specific magnetic susceptibility was determined using Bartington MS2 and MS2B instruments. Analyses of nitrogen, total carbon, and total organic carbon contents were carried out by CNS-Analyser (Elementar Vario EL III).

3.2. Geochronology

In order to understand the age sequence of the late Quaternary deposits exposed on Kurungnakh Island we used different dating methods for several sediment units. Two samples taken in 2000 (Schirrmeister et al., 2001) from two frozen peat layers within the lower sand horizon were dated by isochron uranium–thorium disequilibria technique with a thermal ionisation mass spectrometer (TIMS, Finnigan MAT 262+RPQ) at the Leibniz Institute for Applied Geosciences (GGA, Hannover, Germany). Analytical procedures are described in detail by Schirrmeister et al. (2002c) and Frechen et al. (2007). The external reproducibility was determined by measurements of standard solution of NBL-112A (New Brunswick Laboratories Certified Reference Material) and yields a value of 0.3% (1σ SD).

The radiocarbon dating of handpicked plant remains from a total of 14 sediment samples was performed at the Leibniz Laboratory for Radiometric Dating and Stable Isotope Research, University of Kiel (Germany) using accelerator mass spectrometry (AMS). Details of the AMS procedures at the Leibniz Laboratory are given by Nadeau et al. (1997, 1998). Calibrated ages were calculated using the software "CALIB rev 4.3" (Stuiver et al., 1998).

3.3. Stable isotopes

Ice wedges are common features of periglacial landscapes in non-glaciated regions of Northeast Siberia (Fig. 2). Palaeoclimate studies in polar regions often provide reconstructions of palaeotemperatures and moisture sources using the composition of hydrogen (δD) and oxygen (δ^{18}O) stable isotopes of ice as well as the deuterium excess ($d = \delta D - 8\delta^{18}O$). In this context, ice wedges reflects a winter temperature signal (e.g. Vasil'chuk, 1992; Meyer et al., 2002a, b).

The stable carbon isotope (δ^{13}C) content of TOC was analysed by mass spectrometry (Finnigan Delta S) after removal of carbonate with 10% HCl in Ag-cups and combustion to CO_2 in a Heraeus elemental analyser (Fry et al., 1992). Accuracy of the methods was determined by parallel analysis of international standard reference material. The analyses were accurate to ± 0.2‰. The values are expressed in delta per mil notation (δ, ‰) relative to the Vienna Pee Dee Belemnite (VPDB) Standard.

Ice wedges were sampled for oxygen and hydrogen stable isotope analysis (δD, δ^{18}O) at two sites of the section; the first site (Bkh IW I) within in the upper sequence of the outcrop at 34–35 m a.r.l., and the second site (Bkh IW II) at 16 m a.r.l. (Fig. 3). We used ice screws to drill transects across the exposed ice, keeping a distance of 0.1 m between the drill-holes. Altogether we obtained 14 samples in one transect for stable isotope analysis from the lower site and 15 samples in three levels from the upper sites (Fig. 4). The ice samples were stored cool and afterwards analysed by equilibration technique (Meyer et al., 2000) with a mass spectrometer (Finnigan MAT Delta-S). The reproducibility derived from long-term standard measurements is established with 1σ better than ± 0.1‰ (Meyer et al., 2000). All samples were run at least in duplicate. The values are expressed in delta per mil notation (δ, ‰) relative to the Vienna Standard Mean Ocean Water (VSMOW) Standard.

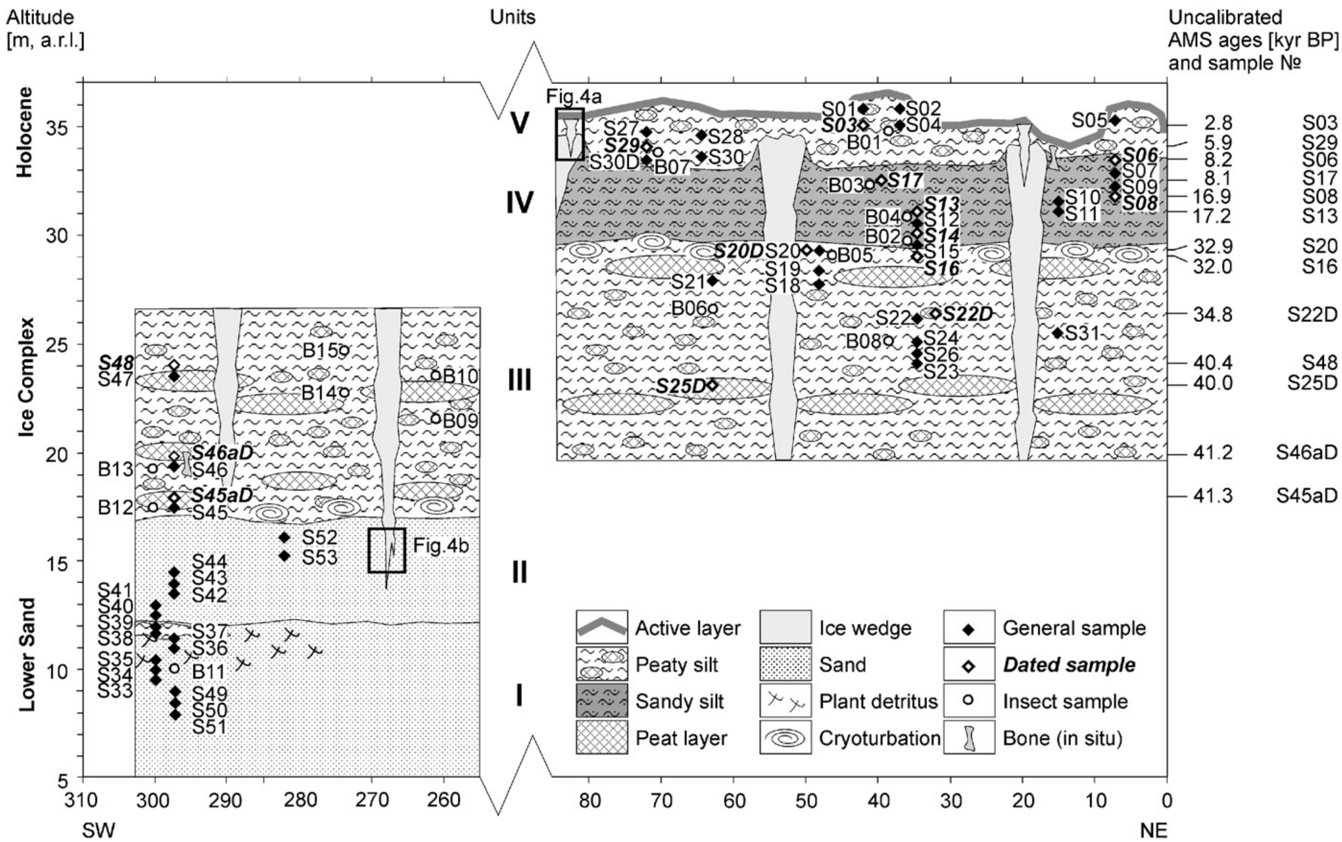

Fig. 3. Scheme of the studied permafrost sequence with sample positions and radiocarbon ages. The position of the additional sampled ice wedges are marked by black frames (see Fig. 4). Note distance of about 150 m between the sections.

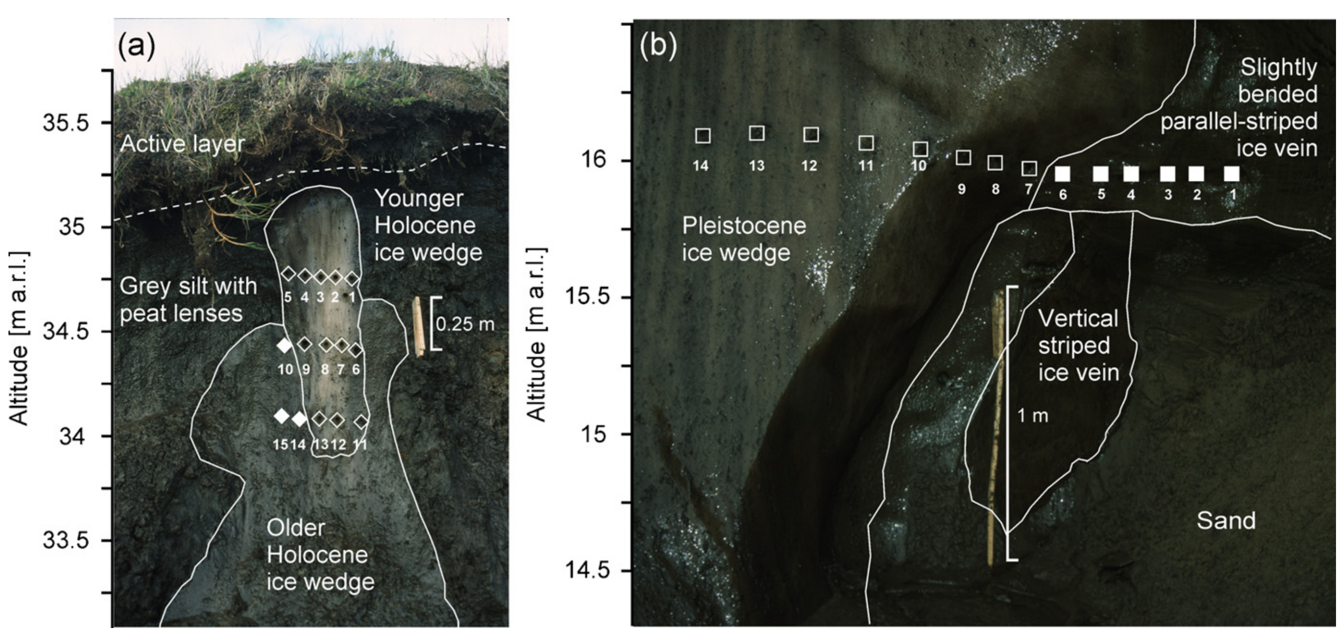

Fig. 4. Sample transects across the studied ice wedges: (a) exposure of two Holocene ice wedge generations (Bkh IW I); (b) Pleistocene ice wedge exposure (Bkh IW II). Filled and open symbols correspond to Fig. 7.

3.4. Palaeoecological proxies

The palaeoecological reconstruction is based on the remains of several bioindicators preserved in the frozen deposits such as pollen, plant macro-fossils, ostracods, insect remains, and mammal bones. These proxies were determined by A. Andreev (pollen), F. Kienast (plant macro-fossils), S. Wetterich (ostracods), S. Kuzmina (insect remains), and T. Kuznetsova (mammal bones).

In total, 18 samples from the radiocarbon-dated units were used for analyses of pollen and palynomorphs. Pollen and spores were identified using a microscope with 400× magnification. Pollen percentages were calculated based on the tree and herbs pollen sum. Pollen zonation was determined by visual inspection. The TILIAGRAPH programme (Grimm, 1991) was used for graphing the pollen data.

For the identification of plant macro-remains and ostracods in the sediments, samples were wet-sieved through a 0.25 mm mesh screen, and then air-dried. About 0.2 kg of each sample was used. If less material was available, the counted numbers of remains were normalised to a 0.2 kg sediment weight. In total, 66 (sub-)-samples were screened for these purposes. Plant macro-remains and ostracod valves were analysed under a stereo-microscope. The species identification of plant remains was based on a carpological reference collection, whereas the ostracod taxa were determined using taxonomical keys (Alm, 1914; Pietrzeniuk, 1977; Meisch, 2000) as well as the reference collection of freshwater ostracods at the Museum of Natural History (Berlin, Germany). For scanning electron microscopy (SEM) photographs of ostracod valves we used a Zeiss DSM 962 at the GeoForschungsZentrum (Research Centre for Geosciences, Potsdam, Germany).

In total, 15 samples of about 50 kg each, mostly taken from thawed sediment, were screened for insect remains. One sample was collected from the lower sequence and 10 samples were taken from the upper sequence. In addition, four samples were screened from two freshly fallen frozen blocks of Ice Complex sediments, which could be assigned to their original position. We used a 0.4 mm mesh sieve for field screening. After drying, the concentrated plant detritus with insect remains was separated using a set of small soil sieves with meshes from 0.25 to 5 mm. The large fraction (2–5 mm) was studied visually; the smaller fractions were analysed under a stereo-microscope. The species identification is based on etalon collections of modern insects from the Zoological Institute of the Russian Academy of Science (RAS), St. Petersburg and the Palaeontological Institute RAS, Moscow, Russia. Photographs of fossil insects were taken at the Otto Schmidt Laboratory, St. Petersburg, Russia. For palaeoenvironmental reconstruction based on fossil insects, we used the Ecological Group Analysis (EGA), which was described in detail in previous works (Sher et al., 2005; Kuzmina and Sher, 2006).

During our fieldwork we also collected mammal bones and their fragments. Afterwards, these fossil remains of the Mammoth Fauna were identified. The bones were obtained: (a) in situ, i.e. within the frozen sediment, (b) in thermo-erosional cirques, where the original position within the sediments can be determined, (c) within the thawed debris of the outcrop, and (d) on the Lena River bank. Two of these bones were used for radiocarbon dating at the Geological Institute (GIN) of the RAS in Moscow and at the Oxford Radiocarbon Accelerator Unit Research Laboratory (OxA).

4. Results

4.1. Lithostratigraphy, sedimentology, and cryolithology

In general the cliffs along the Olenyeksky Channel consist dominantly of a lower, sandy and ice-poor formation (units I and II) and an upper ice-rich, fine-grained, peaty formation (Ice Complex), which contains numerous large ice wedges (units III and IV), and which are overlain by thermokarst depression fillings (unit V). Because of quite similar cryostructures in upper ice-rich formation and partly problematic exposure conditions (steep, slippery muddy, many debris) boundaries between the separate units were not always very well visible during the field observation. Nevertheless, our sedimentological data from the deposits of Kurungnakh Island confirm the stratigraphical division of the exposure into five main units (Fig. 5; Table 1), which was made during the field work. The deposits of the lower sand sequence are well exposed along the whole section. The sands reach altitudes up to 17 m a.r.l. and delineate a division by sedimentological parameters into two units (Fig. 5).

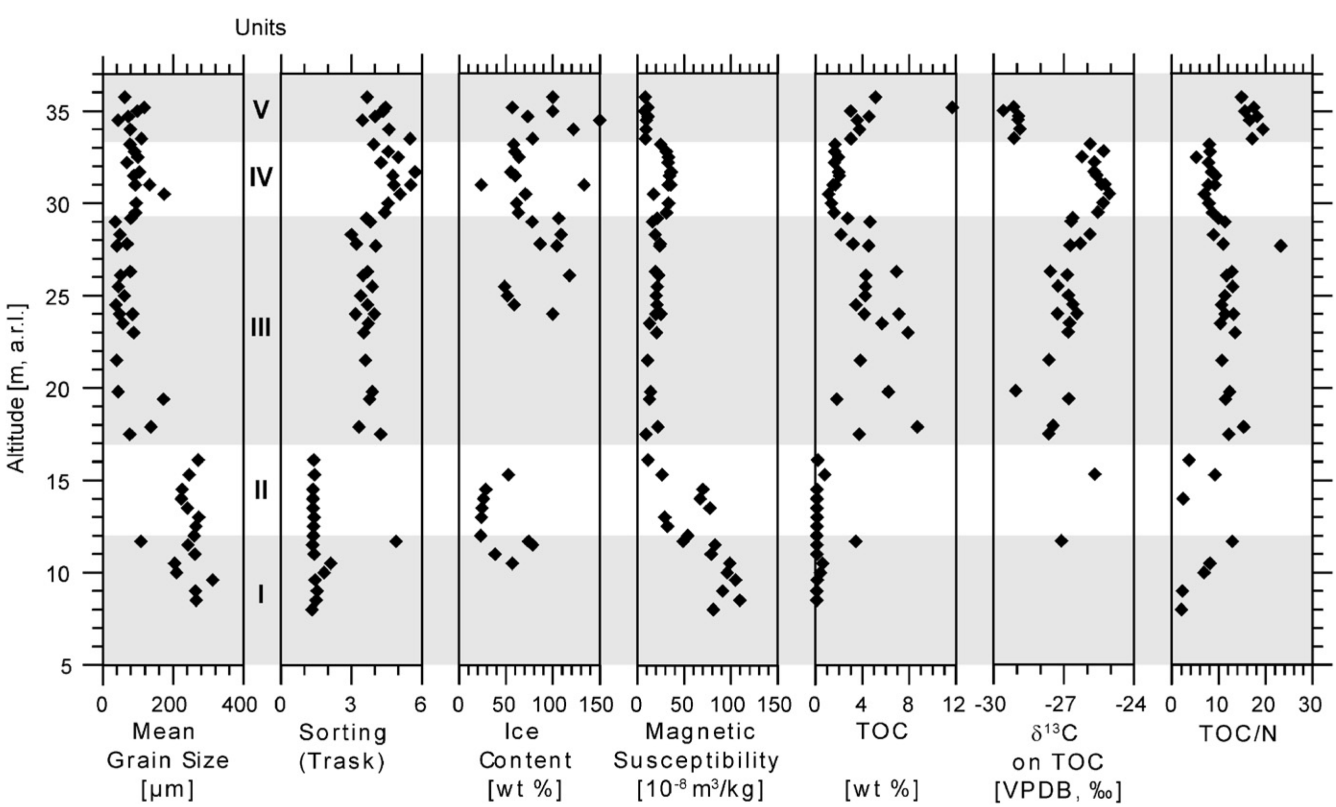

Fig. 5. Stratigraphic differentiation of the permafrost sequence into units I–V according to sedimentological records.

Table 1
Stratigraphic composition of the studied permafrost sequence and sediment characteristics of individual sediment units

Unit	Altitude (m a.r.l.)	AMS-ages (kyr BP)	Stratigraphy	Sediments
V	33.5–37	6–3	Middle and late Holocene	Grey peaty silt with peat lenses and the uppermost modern active layer
IVb	32–33.5	About 8	Early Holocene Gap	Grey sandy silt with rare plant detritus
IVa	29.5–32	About 17	Late Weichselian Stadial (Sartan) Gap	Grey sandy silt with rare plant detritus
III	17–29.5	42–32	Middle Weichselian Interstadial (Kargin)	Grey peaty silt as continuous Ice Complex deposits with peat lenses and layers, including cryoturbated palaeosol horizons
II	12–17	>50	Early Weichselian Stadial (Zyryan)	Yellow medium-grained homogeneous finely laminated pure sand
I	Up to 12	> 50	Early Weichselian Stadial (Zyryan)	Interbedded yellow medium-grained sand and grey silty sand with plant detritus, roots and single silt layers

4.1.1. Unit I (up to 12 m a.r.l.)

Unit I consists of interbedded yellow medium-grained sand (1–5 cm thick) and grey silty sand (1–2 cm thick) with plant detritus, roots, and single silt layers (Appendix A in Supplementary data). In some layers of unit I, the sands contain abundant grass roots and stems. Well-sorted medium-grained sands with low TOC and TOC/N ratios alternate with poorly sorted silty sands with higher TOC and TOC/N ratios. This interbedding reflects frequent changes in the current velocity under shallow water conditions. The ice content is generally lower in coarser sediments (about 25 wt%). No ice wedges were observed within unit I. The cryostructure is massive, i.e. no distinct small-scale segregated ice lenses or veins were visible. The magnetic susceptibility decreases from more than 100×10^{-8} m^3/kg at about 9 m a.r.l. to less than 50×10^{-8} m^3/kg at the transition to unit II.

4.1.2. Unit II (12–17 m a.r.l.)

Above the alternation of sand, silt and plant detritus layers in unit I the upper part of the sand formation was characterised by homogeneous finely laminated pure sand (Appendix A in Supplementary data). Single laminae of grey, greyish, and light-brown colour are 0.2–2 cm thick partly with graded bedding structures. The boundary between units I and II was not very sharp and hardly identifiable. Deposits of unit II are well-sorted medium-grained sands and contain only very little organic material (TOC 0.12–0.19 wt%) (Fig. 5). Thin layers of fine plant detritus were only observed in some places. The fine lamination was synsedimentarily disturbed at the mm-scale (load casts). Sediment features reflect that fluvial accumulation conditions changed to more continuous transport in rather shallow water. The general trend of decreasing magnetic susceptibility continues in unit II. The ice content varies between 23 and 26 wt%. The cryostructure is massive without any small-scale structures of segregated ice. No syngenetic ice wedges were formed. But epigenetic thin ice wedges, which form the "roots" of the large ice wedges in unit III penetrate the upper part of unit II.

4.1.3. Unit III (17–29.2 m a.r.l.)

The upper sand sequence of unit II is covered by the Ice Complex sequence. The boundary between the lower sand and the Ice Complex is sharp and visible along the whole section (Fig. 2). At this boundary an approximately 1-m-thick horizon of a cryoturbated palaeosol occurred. Ice Complex ice wedges sharply narrow near the boundary with the lower sand sequence, and their long and thin tails penetrate about 1–2 m into the sand unit II. The Ice Complex is often exposed in the form of an ice wall along the river bank (Fig. 2). This wall, up to 1 km long, is likely the longitudinal part of a polygonal ice wedge system. The ice wall is covered by overhanging frozen blocks of peat and silt (Fig. 2). In less steep parts of the outcrop numerous thermokarst mounds reflect the transversal cut through a polygonal ice wedge system (Appendix A in Supplementary data). The thickest peat layers are observed in the lower part of the Ice Complex sequence (unit III). At least two such layers are clearly observed along the section. In addition, cryoturbated greyish-brown palaeosols of about 0.5 m thickness with peat inclusions and twig fragments occurred repeatedly within unit III. The described characteristics reflect the subaerial accumulation of these sediments.

Unit III is composed of ice-rich poorly sorted, cryoturbated greyish sandy silt with 0.5–0.7 m thick peat horizons, single sand and peat lenses (0.2–0.5 m in diameter), and large ice wedges (Figs. 3 and 5). The ice wedges are 2–4 m wide and 15–20 m high. They have symmetrical shoulders, which merge to ice bands (segregation ice). Such ice wedges are vertically striped, consist of numerous 1–2 cm thick elementary ice veins, and contain numerous small gas bubbles. The ice content in sediments of unit III varies from 50 to 133 wt%. Ice bands of 1–3 cm thickness as well as reticulate nets of mm-thin ice veins and lenses between the ice bands characterise the cryostructure. The shape of the large wedges and their connection to the bands of segregated ice band as well as the ice supersaturation are signs of syngenetic (i.e. contemporary) ice wedge growth and accumulation. The magnetic susceptibility shows a stable signal of about 20×10^{-8} m^3/kg. The TOC content of these organic-rich sediments ranges from about 2 to 7 wt%, and the TOC/N ratio varies from about 9 to 23. The δ^{13}C averages about -27‰.

In the upper part of the Ice Complex sequence the peat layers are rare and less thick. The boundary to the overlain unit IV is again formed by a cryoturbated palaeosol of 0.5–1.5 m thickness. There, sandy layers or lenses are often observed near the contact between ice wedges and the surrounding sediments.

4.1.4. Unit IV (29.5–33.5 m a.r.l.)

According to field observations unit IV could be separated from the underlain unit III because of yellowish grey to greenish-grey colour, higher sand content, a lack of peat inclusions, and the lesser content of plant remains (only few thin grass roots; Appendix A in Supplementary data). Unit IV is composed of very poorly sorted sandy silt with low organic content. The TOC is significant lower than in unit III (1.7–2 wt%). The δ^{13}C composition of unit IV is clearly shifted to more positive values averaging about -25.5‰ and reaching at its most

Table 2
Data of ^{230}Th/U age determinations of two samples (three subsamples each) from two peat horizon within unit I taken in 2000 (Schirrmeister et al., 2001)

Sample no TIMS no	Altitude (m a.r.l.)	^{234}U/^{238}U $\pm 2\sigma$	^{230}Th/^{232}Th $\pm 2\sigma$	U conc. (ppm)	Th conc. (ppm)	^{230}Th/U age 10^3 yr $\pm 2\sigma$	^{230}Th/U age 10^3 yr $\pm 2\sigma$ Isochrone-corr.
Bkh2 U/Th-1	3.2–3.4						107 ± 3
700		1.181 ± 0.003	0.566 ± 0.003	0.83	5.19	315 ± 10	104 ± 5
701		1.241 ± 0.005	0.7726 ± 0.004	1.50	6.37	194 ± 3	105 ± 3
702		1.194 ± 0.005	0.608 ± 0.005	0.66	3.98	343 ± 21	114 ± 6
Bkh2 U/Th-2	3.6–3.8						95 ± 4
704		1.141 ± 0.003	0.550 ± 0.004	0.66	4.30	457 ± 60	94 ± 8
705		1.241 ± 0.002	0.651 ± 0.004	1.08	5.79	234 ± 4	94 ± 6
706		0.98 ± 0.005	0.546 ± 0.005	0.62	3.52	> 650	99 ± 9

Table 3
Radiocarbon AMS ages of plant remains in samples of the Kurungnakh study site collected in 2002

Sample no.	Lab no.	Material dated	Altitude (m a.r.l.)	Uncal. AMS ages (yr BP)	cal AMS ages[a] (yr BP) Max	cal AMS ages[a] (yr BP) Min
Bkh2002 S03	KIA31046	Plants	35	2795 ± 30	2954	2841
Bkh2002 S29	KIA31047	Plant detritus	34	5860 ± 35	6756	6593
Bkh2002 S06	KIA31048	Plants	33.2	8155 ± 45	9155	9010
Bkh2002 S17	KIA31049	Plants	32.5	8075 ± 30	9034	8980
Bkh2002 S08	KIA30235	Wood	31.7	16 860 ± 70	20 195	19 855
Bkh2002 S13	KIA31050	Plants	31	17 200 ± 80	21 138	19 849
Bkh2002 S14	KIA31051	Plants (relocated)	30	665 ± 30	602	558
Bkh2002 S20	KIA30236	Wood	29.2	32 920+330/−310		
Bkh2002 S16	KIA30237	Wood	29	31 960+380/−360		
Bkh2002 S22D	KIA30238	Wood, leaves	26.3	34 830+390/−370		
Bkh2002 S48	KIA30240	Wood	24	40 410+610/−560		
Bkh2002 S25D	KIA30239	Wood, moss, coarse leaves	23	40 020+660/−610		
Bkh2002 S46aD	KIA30241	Moss, leaf fragments	19.8	41 220+1260/−1090		
Bkh2002 S45aD	KIA31052	Plants	17.9	41 330+2000/−1600		

[a] Calibrated ages were calculated using the software "CALIB rev 4.3" (Stuiver et al., 1998).

positive (heaviest) a value of −25.1‰. The TOC/N ratio in unit IV does not clearly differ from that of unit III. As far as observable the large ice wedges of unit III seemed to continue in unit IV without any interruption. The cryostructure is similar to those of unit III and the ice content is variable (24–150 wt%). The magnetic susceptibility is higher as compared to the overlying unit V and the underlying unit III with values of $17.4–36 \times 10^{-8}$ m^3/kg.

4.1.5. Unit V (33.5–37 m a.r.l.)

The uppermost part of the outcrop below the active layer consists of sandy silt with peat lenses 0.1–0.2 m in diameter (Appendix A in Supplementary data). This deposits form separate, several decametres wide bodies of thermokarst depressions fillings on top of the underlain ice-rich deposits. The contact next to the thick Pleistocene ice wedges between the surrounding sediments of units V and IV is turned up (Fig. 3) indicating the particular erosion (thermokarst) of the upper part of unit IV sediments. Ice wedges of 0.5–1.5 m width and up to 5 m height often penetrate into the much larger ice wedges of unit IV (Fig. 4a) forming larger composite ground ice bodies, which consist of several separate ice wedges. The cryostructure is similar to the ice-rich units below. The ice content of frozen sediments ranges from 48 to 117 wt%. The TOC content is similar to that of unit III and varies between about 3 and 12 wt%. The δ^{13}C signal of unit V clearly differs from all other units and reaches at its most negative (lightest) a value of about −29‰. The TOC/N ratio of about 17 in unit V is significant higher than in the other units. The mass-specific magnetic susceptibility reaches only $8.4–11.5 \times 10^{-8}$ m^3/kg.

4.2. Geochronology

New ^{230}Th/U data from peat layers of unit I show isochron derived mean ages of 107 ± 3 and 95 ± 4 kyr at 3.2–3.8 m a.r.l. (Table 2). Peat layers in similar position in the western Lena Delta exposed about 5 m a.r.l. at the Anrynsky Channel were ^{230}Th/U dated at 113 ± 14 kyr (Schirrmeister et al., 2003). Krbetschek et al. (2002) provided three age determinations between 4.3 and 8.8 m a.r.l. by Infrared Optical Simulated Luminescence (IR-OSL) from 88 ± 14 to 65 ± 8 kyr.

The radiocarbon ages (Table 3) of unit III range between 41.3 +2.0/−1.6 kyr BP at 17.9 m a.r.l. and 32.9 ± 0.3 kyr BP at 29.2 m a.r.l. One dating from this unit (Bkh2002 S14; 665 ± 30 yr BP at 30 m a.r.l.) was excluded from further interpretation, because it comes from relocated material of late Holocene age. In unit IV two ages of about 17 kyr BP were determined at 31 and 31.7 m a.r.l., and two early Holocene ages of about 8 kyr BP at 32.5 and 33.2 m a.r.l. According to these results unit IV should be divided into two subunits IVa and IVb (Table 1). The uppermost unit V was formed during the middle Holocene between about 6 and 3 kyr BP.

In order to understand the complete radiocarbon geochronology of the studied section we combined our new results with previous radiocarbon data from Schirrmeister et al. (2003) (Fig. 6a); the good agreement of these two studied outcrops on Kurungnakh Island is apparent. Considering the total data set of 28 radiocarbon ages it has to be mentioned that two gaps in the chronology are present between approximately 32 and 17 kyr BP and between 17 and 8 kyr BP. The continuous sedimentation between about 50 and 32 kyr BP (during the Middle Weichselian/Kargin/MIS-3 interstadial) allows us to estimate an age–height correlation ($R^2_{mean} = 0.87$) based on 11 dates for this period (Fig. 6b). This good correlation was also used in palaeoecological studies for age estimations of non-dated samples.

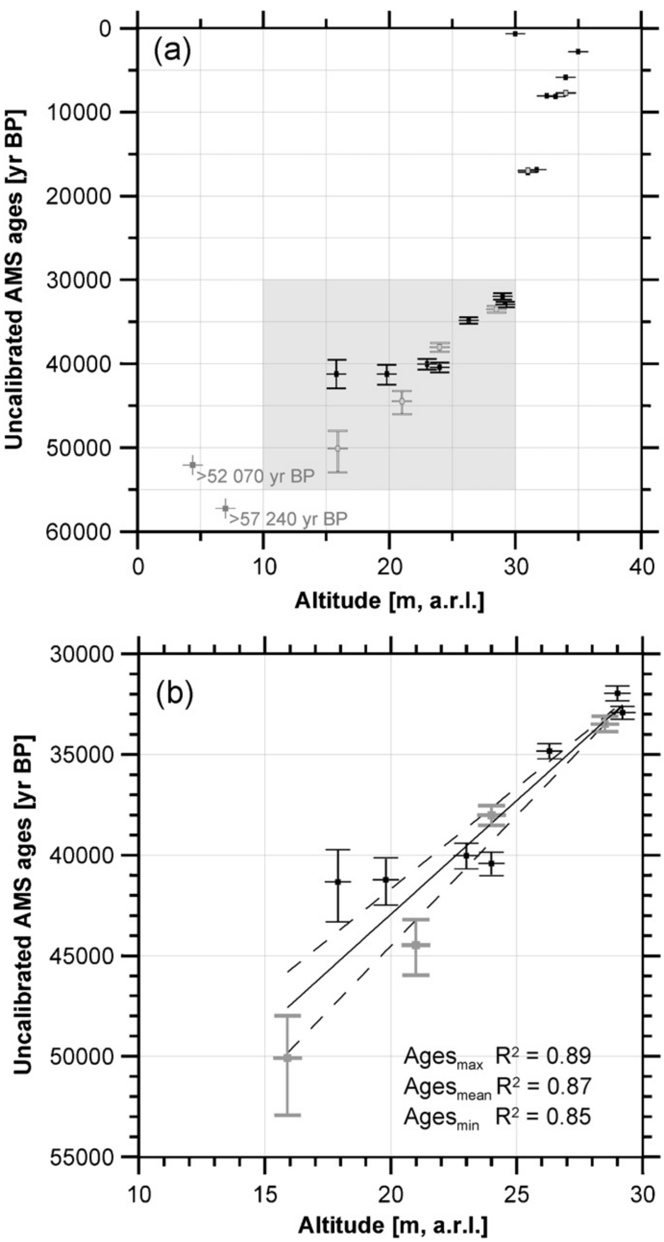

Fig. 6. Results of radiocarbon AMS age determination from Kurungnakh Island: (a) age-model of the entire radiocarbon-dated permafrost sequence; (b) age–altitude-correlation of the continuously accumulated Kargin period between 50 and 31 kyr BP. Previous dates from Schirrmeister et al. (2003) are marked as grey symbols.

4.3. Oxygen and hydrogen stable isotopes of ground ice

The studied late Pleistocene ice wedge is about 2 m wide at the sample site and penetrates another 2 m further into unit II. The sampled transect covers the right side of a large ice wedge (samples Bkh-II 7–14) and a smaller, slightly bended parallel-striped ice vein (samples BKh IW II 1–6), which merges oblique into the ice wedge (Fig. 4b). Such kind of small "daughter ice wedges" was often observed in the lowermost part of large ice wedges. They mirror changing frost crack orientation during epigenetic ice wedge formation if stress relations during frost cracking were not yet clear. The apparently horizontal orientation of such ice wedge is caused by angular cutting orientation of the inclined oriented ice body. Two small Holocene ice wedges that nest one into another (Bkh IW I) were sampled at the top of the section (Fig. 4a).

The stable isotope signature of late Pleistocene ice lies in a more negative (lighter) range of about −32‰ for $\delta^{18}O$ and −248‰ for δD, whereas the *d* excess averages 6‰ (Table 4). The horizontally striped ice vein next to this ice wedge is slightly shifted to heavier values of −31‰ for $\delta^{18}O$ and −241‰ for δD ($d \approx 4‰$).

The younger Holocene ice wedge shows relatively heavy values of around −25‰ for $\delta^{18}O$ and −185‰ for δD. The *d* excess averages about 12‰ (Table 4). This is clearly different from the surrounding older Holocene ice in which the younger ice wedge grew, with values of about −25‰ for $\delta^{18}O$, −199‰ for δD, and 4‰ for the *d* excess (Table 4). The $\delta^{18}O$-δD signature of the older Holocene ice wedge lies below the Global Meteoric Water Line (GMWL; Fig. 7). The relatively low *d* excess is not typical for Holocene ice wedges and might indicate that this generation of ice wedges formed not only under the influence of winter snow, but also were fed by additional water supply. However, these samples are less suitable for climate interpretation.

In summary, late Pleistocene and Holocene ground ice are clearly differentiated by their stable isotopic signals. Similar results have been obtained from other outcrops in the Laptev Sea region (Meyer et al., 2002a, b; Schirrmeister et al., 2003). The interpretation of the stable isotope data allows us to conclude that winter temperatures were warmer during the late Holocene than in the late Pleistocene when the Ice Complex formed.

4.4. Palynological studies

Sediments of units I and II contain almost no pollen. Five pollen zones (PZ 1–5) can be distinguished in units III–V (Fig. 8). The dominance of Cyperaceae and Poaceae pollen with some *Artemisia* and *Salix* is typical for pollen zone 1 (PZ 1) corresponding to the lower part of unit III (ca 45–40 kyr BP). The pollen spectra reflect the domination of open tundra- and steppe-like associations in the area at that time, although willow shrublets were probably present in the vegetation as well. A relatively high content of green algae colonies (*Pediastrum*) indicates the existence of shallow water bodies (e.g. centres of ice wedge polygons). The interval corresponds well with the beginning of the Kargin interstadial when climate amelioration took place.

Table 4
Oxygen and hydrogen table isotope signatures of late Pleistocene and Holocene ice wedges

Type of ground ice	Sub-samples	Altitude (m a.r.l.)	$\delta^{18}O$ mean (‰)	$\delta^{18}O$ std. dev. (‰)	δD mean (‰)	δD std. dev. (‰)	*d* mean (‰)	*d* std. dev. (‰)
Younger Holocene ice wedge	12	34–35	−24.6	0.8	−185.1	6.1	11.6	1.0
Older Holocene ice wedge	3	34–35	−25.4	1.1	−198.6	7.0	4.2	1.7
Late Pleistocene ice wedge	8	16	−31.8	0.5	−248.3	3.2	5.8	0.4
Horizontal striped ice vein	6	16	−30.6	0.5	−240.7	3.4	4.0	0.7

The dominance of Poaceae, Cyperaceae, *Artemisia*, and Caryophyllaceae pollen with some Asteraceae, *Thalictrum*, and Brassicaceae is typical for PZ 2 corresponding to the upper part of unit III (ca 40 and 32 kyr BP). This interval corresponds well with the climatic optimum of the Kargin interstadial. The pollen spectra reflect the domination of open steppe-like and tundra-like associations in the area at that time. Relatively high contents of *Pediastrum* and *Botryococcus* colonies and *Salix* pollen indicate relatively moist local conditions during this interval. A similar environment was reconstructed for this time for the Bykovsky Peninsula, Laptev Sea (72°N, 129°E; Fig. 1) as well (Andreev et al., 2002; Schirrmeister et al., 2002a). Large amounts of spores from dung-inhabiting Sordariales fungi (*Sporormiella*, *Podospora*, and *Sordaria*) are also characteristic for the spectra, and can be seen as an indication of grazing mammals in the area during that time.

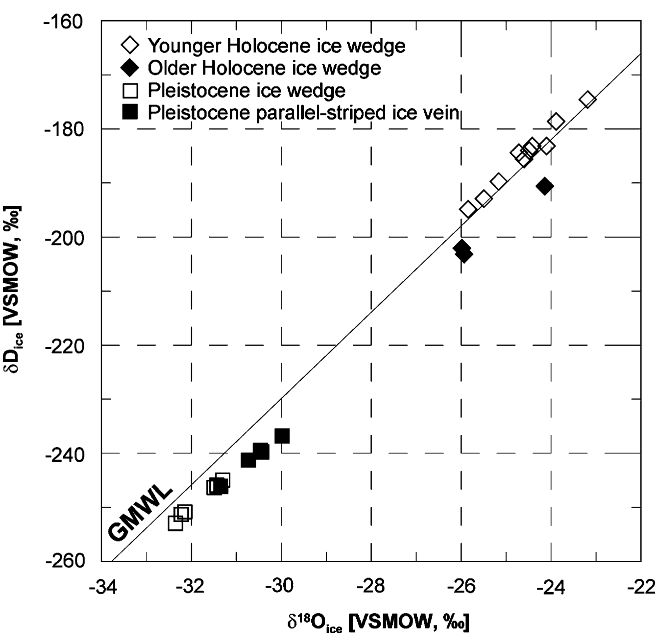

Fig. 7. δ^{18}O–δD plot of Pleistocene and Holocene ground ice as with respect to the Global Meteoric Water Line (GMWL), which correlates fresh surface waters on a global scale (Craig, 1961).

Very low pollen concentrations characterise PZ 3 (unit IVa) dated at around 17 kyr BP. This feature may indicate scarce vegetation around the site, or more likely very low pollination during the Sartan stage. Pollen spectra are dominated by Poaceae, Cyperaceae, *Artemisia*, and Caryophyllaceae. They also contain reworked indeterminable Pinaceae pollen grains and rather numerous dung-inhabiting fungi spores. The latter most likely indicate the presence of grazing herds in the area. It can be assumed that scarce steppe-like grass-sedge-*Artemisia* communities dominated the study area. The climate was probably extremely cold and dry. However, relative high contents of *Betula* sect. *Nanae* and *Salix* pollen may reflect the beginning of slight climate amelioration after the Last Glacial Maximum (LGM).

An increase in *Alnus fruticosa*, *Betula* sect. *Nanae*, *B.* sect. *Albae*, and Ericales pollen contents and the presence of *Rubus chamaemorus* in PZ 4 reflect the early Holocene warming (unit IVb). Such changes suggest that shrubby tundra was widely distributed around the site ca 8 kyr BP. Previous studies at the area confirm this conclusion (Schirrmeister et al., 2003). The second spectrum of PZ 4 (unit V) radiocarbon dated to 5.9 kyr BP is characterised by a strong decrease in *A. fruticosa* and increase in *Betula nana* and Ericales pollen. These changes reflect some climatic deterioration resulting in the disappearance of shrub alder from the vegetation.

The uppermost spectrum of PZ 5 (unit V) radiocarbon dated to ca 2.5 kyr BP is characterised by a disappearance of Ericales and *R. chamaemorus* pollen, and an increase in *Salix*, Cyperaceae, and long-distance transported pollen (*Pinus*). The spectrum reflects vegetation and climate conditions similar to modern.

4.5. Plant macro-fossils

In general, the studied sequence is poor in plant macro-fossils. Altogether 66 samples were studied of which only 42 contained identifiable material (Appendix B in Supplementary data).

In the lowermost units I and II, plant macro-remains were especially rare. Both units are similar in their fossil plant composition. The macro-fossil spectra include beside *Salix* sp., and *Carex* sp. mainly tundra–steppe representatives like *Potentilla* sp., *Kobresia myosuroides*, *Puccinellia* sp. but also wetland species such as *Carex* sect. *Phacocystis*, *Saxifraga hirculus*, and *Eriophorum angustifolium* (Fig. 9). They reflect a tundra–steppe-like vegetation,

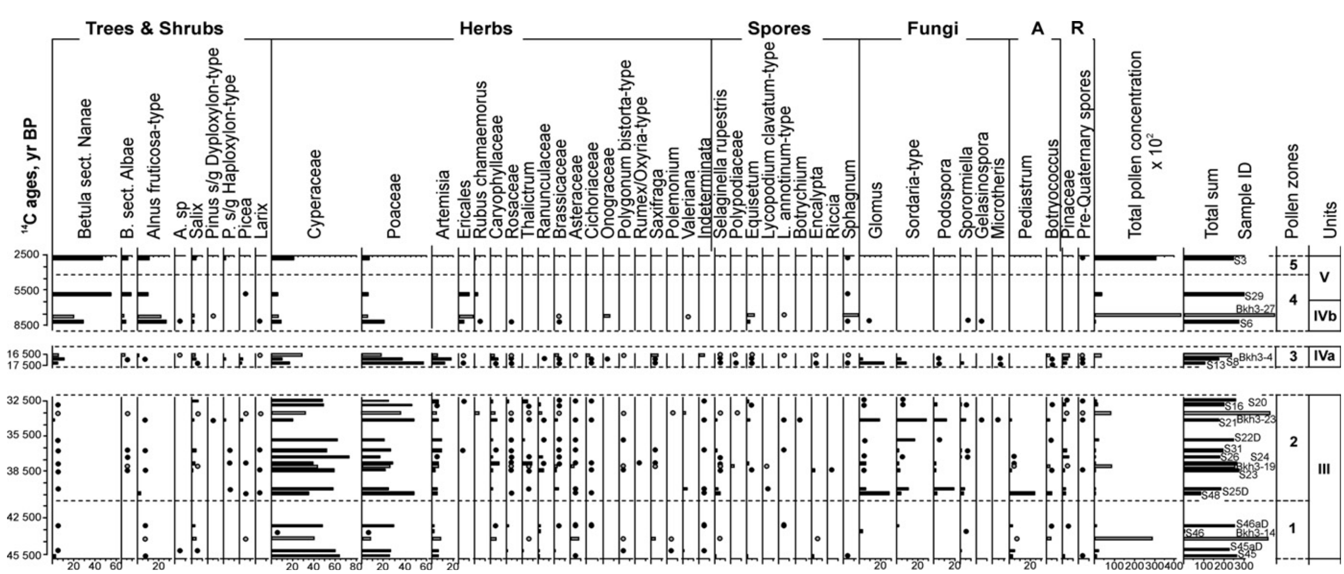

Fig. 8. Pollen and spore diagram of Kargin, late Sartan and Holocene sediments (A—algae remains, R—re-deposited taxa). Pollen and spore data from Schirrmeister et al. (2003) are marked as grey bars and dots.

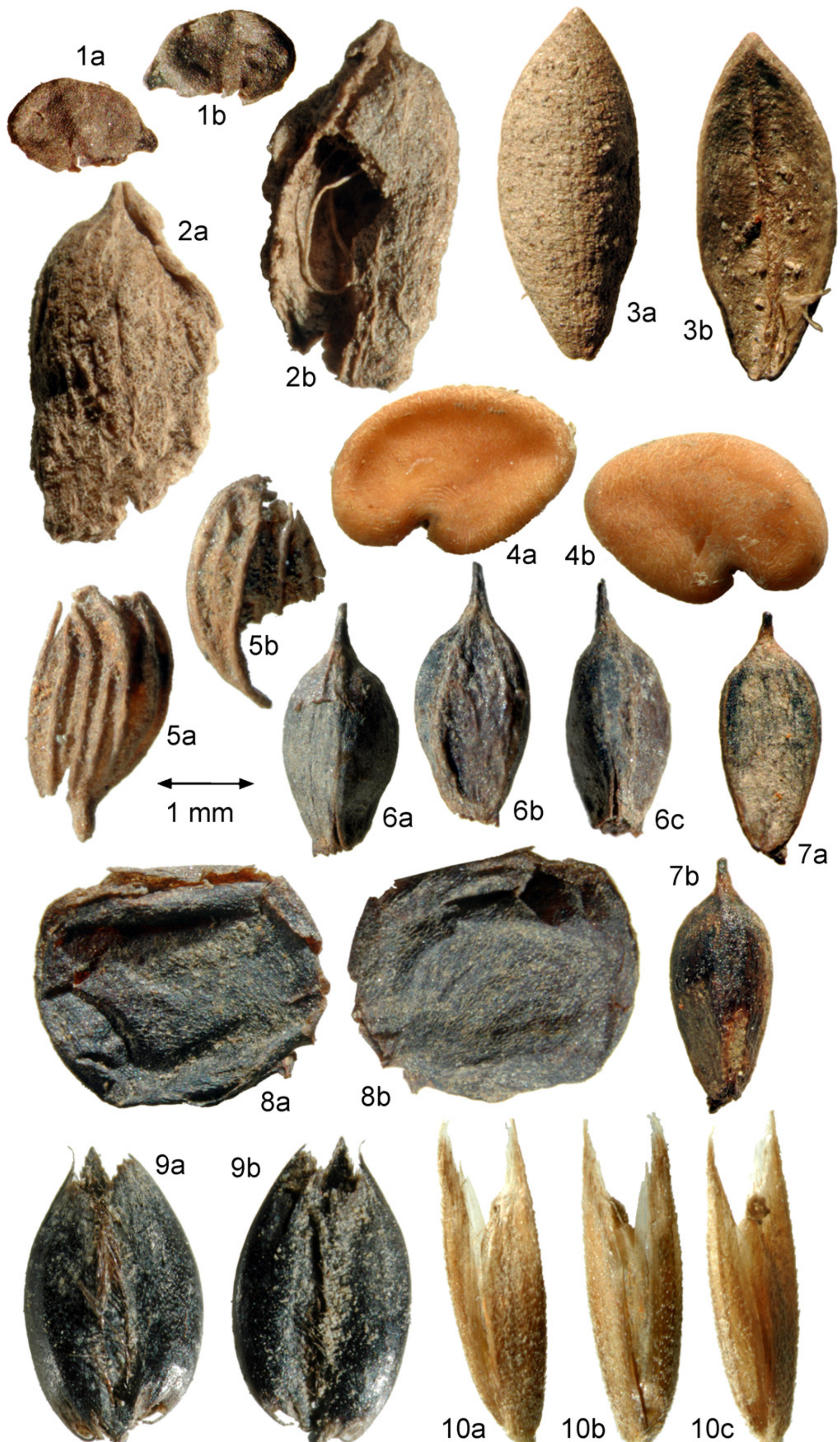

Fig. 9. Fossil plant macro-remains from Kurungnakh Island: (1) *Alyssum obovatum*, both sides of a seed fragment; (2) *Lagotis minor*, fragment of the fruit, two sides; (3) *Phlox sibirica*, valve of the capsule, two-sided; (4) *Astragalus* sp., both sides of the seed; (5) *Thalictrum alpinum*, fragments of two individual pericarps; (6) *Kobresia myosuroides*, three sides of a nutlet; (7) *Kobresia myosuroides*, two sides of another nutlet; (8) cf. *Lesquerella arctica*, seed, two-sided; (9) *Hierochloë* cf. *odorata*, spikelet with two visible staminate florets enclosing one pistillate floret, two sides; (10) *Arctagrostis latifolia*, caryopsis, (a) and (b) lateral, (c) obliquely ventral view showing that the peduncle is lacking (evidence that spikelets are uniflorous).

thus cold and dry conditions and the presence of wet localities. The scarcity of plant remains is likely the result of taphonomical conditions and is not regarded as being due to climatic conditions. Well-sorted sand is deposited by wind or running water, implicating the removal of lightweight fractions of the sediment load including small grain sizes and plant detritus.

Unit III consists mainly of organic-rich silty and peaty deposits, which inherently contain more identifiable plant remains. Consistently, the diversity and abundance of plant macro-remains in unit III are the highest within the recorded sequence. The spectra are mainly dominated by artic upland plants characteristic of *Kobresia* meadows and by steppe plants (Appendix B in Supplementary data), reflecting the presence of a tundra–steppe under dry conditions. Remains of *Carex* sect. *Phacocystis* were also abundant, indicating the existence of constantly wet habitats possibly connected with periodic flooding in the proximity of a riverbed. The nearby existence of a river bed might also explain the scarcity of *Puccinellia* sp., a plant species that is actually very abundant in Pleistocene deposits of Arctic Siberia (Kienast et al., 2005, 2008). This grass occurs inland only under dry climate conditions in closed depressions, which lack drainage, where groundwater level and salt concentration fluctuate seasonally due to high evaporation. The high drainage that exists close to a river bed probably hampered salt accumulation in the top soil.

In unit IVa, the composition of the macro-fossil assemblages does not change significantly from that of unit III, but the abundance and diversity of plant remains decrease (Appendix B in Supplementary data). This might be the result of a higher accumulation rate or of poor macro-fossil preservation. Since all palaeoecological records indicate a drastic decrease in diversity and abundance and a dominance of cold-tolerant taxa, a strong temperature decrease has to be assumed.

Interestingly, the floral composition does not change notably towards the early Holocene warming (unit IVb). Plants typical of the Pleistocene tundra–steppe such as *K. myosuroides* and *Potentilla* cf. *stipularis* continue to exist in the study area beyond the Weichselian/Holocene border. Their existence together with the low number of wetland plants during the early Holocene might be an indication of a continuing continental climate as a result of delayed Laptev Sea transgression. Plant remains indicating a temperature increase towards the early Holocene are largely absent except for a single Betulaceae fruit in the Bkh2002 S30D sample. This result is in contrast to palynological results, which clearly show a drastic increase in *A. fruticosa*, *Betula* sect. *Nanae*, *B.* sect. *Albae*, and Ericales pollen.

Unit V corresponds largely to the late Holocene and is characterised by a further floral impoverishment connected with increasing oceanic climate influence due to the Laptev Sea transgression. Among the few macro-fossils that were found, remains of wetland sedges (*Carex* sect. *Phacocystis*) and willow shrubs dominate. Single remains of *Betula* cf. *fruticosa* and *Ledum palustre* indicate subarctic temperature conditions. Steppe, meadow, and cryo-arid elements are completely absent from the late Holocene record.

4.6. Ostracod remains

In total, 54 samples from the site studied in 2002 and 15 samples from the outcrop sampled in 2000 were checked for ostracod remains. However, only five samples from the 2000 and 2002 sample sets contained any ostracod remains, mostly rare valve fragments or single valves of juvenile Candoninae and *Candona muelleri jakutica*. The only sample with sufficiently high valve numbers (in total 2485 valves) for further interpretation was found at an altitude of 19.8 m a.r.l. (sample Bkh2002 S46aD) in the lower part of unit III. This sample was dated to 41 220+1260/−1090 yr BP. The species composition comprises five taxa. Four species were identified by valves of adult specimens and one taxon comprises juvenile Candoninae, which represents more than 50% of the total amount of ostracod valves. The abundance of the four species is shown in Fig. 10. Due to finding only four species represented by adults the species diversity is low. Nevertheless, some interpretation can be undertaken. All observed species are already described for modern (sub-)arctic shallow water habitats (e.g. Alm, 1914; Semenova, 2003, 2005; Wetterich et al., 2008). The good preservation of the valves which even contain, in some cases, soft body parts, and also the occurrence of closed carapaces indicate in situ conditions (Fig. 11).

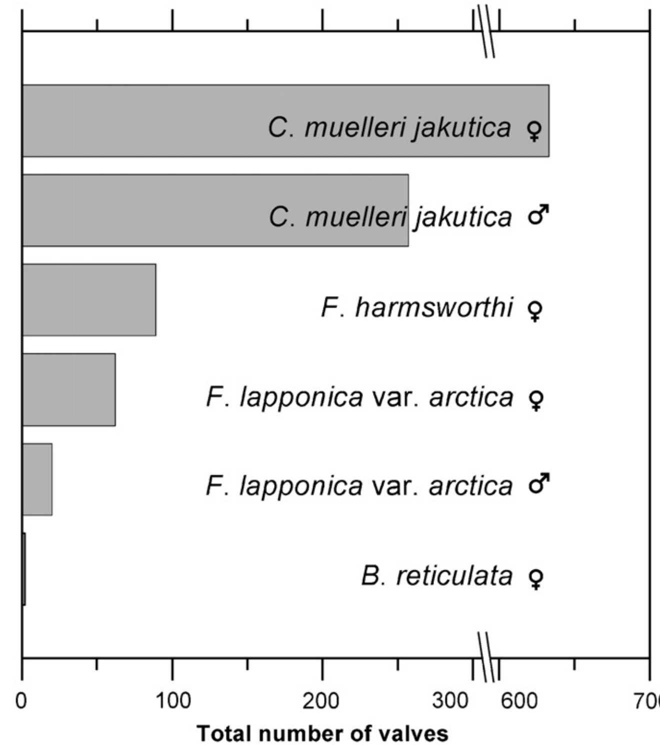

Fig. 10. Ostracode species spectra of sample Bkh2002 S 46 aD (19.8 m a.s.l.) in the lower part of unit III dated to 41 kyr BP.

The most common species in the record here presented is *C. muelleri jakutica* Pietrzeniuk, 1977 (Fig. 11, pp. 1–4) which was first observed in Central Yakutian thermokarst lakes (Pietrzeniuk, 1977) and has also been found in arctic polygonal ponds in the Lena Delta (Wetterich et al., 2008) under very low electrical conductivities (salinities) and water temperatures between about 5 and 15 °C. Fossils of *C. muelleri jakutica* are already known from Kargin interstadial deposits from Bykovsky Peninsula, Laptev Sea, Northeast Siberia (Wetterich et al., 2005). Modern and fossil assemblages of *C. muelleri jakutica* are commonly represented by female and male specimen.

The species *Fabaeformiscandona harmsworthi* (Scott, 1899) (Fig. 11, pp. 5–6) has been found in the modern arctic environments of Novaya Zemlya and Franz Josef Land (Neale, 1969) and also in the Lena Delta under the same environmental conditions as *C. muelleri jakutica* (Wetterich et al., 2008). Fossil valves were obtained in Kargin interstadial deposits in Northeast Siberia (Wetterich et al., 2005). Only female *F. harmsworthi* valves have been found. Males are not known.

Fabaeformiscandona lapponica var. *arctica* (Alm, 1914) (Fig. 11, pp. 7–10) was first described from ponds on Novaya Zemlya Archipelago, Russian Arctic (Alm, 1914). Semenova (2003) classified

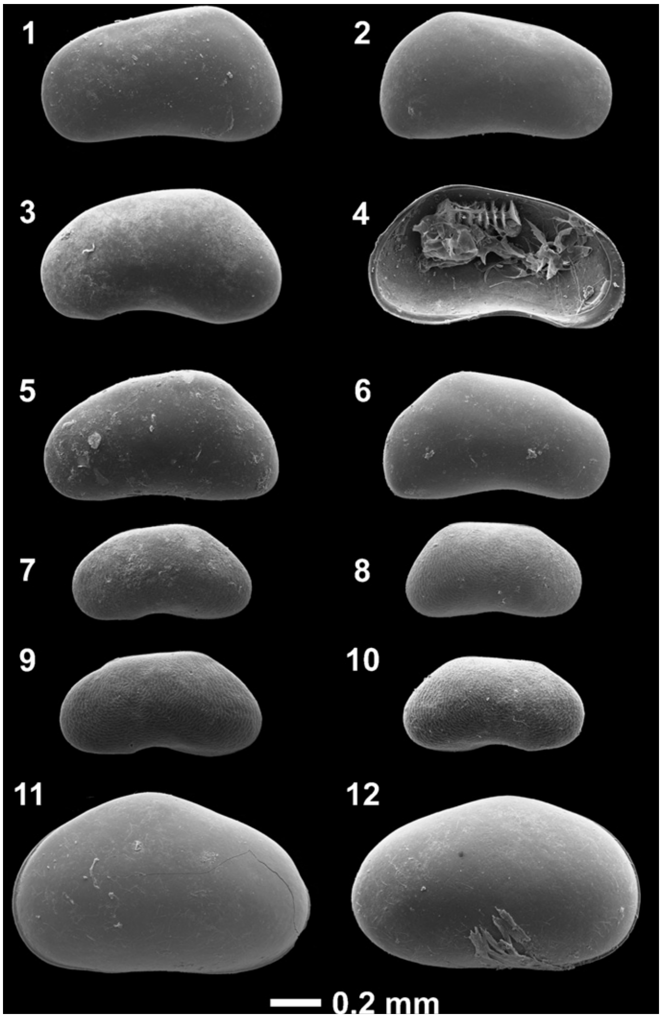

Fig. 11. SEM photography of freshwater ostracod valves (left valve—LV, right valve—RV). *Candona muelleri jakutica*: (1) female LV, (2) female RV, (3) male LV, (4) male LV (internal view with preserved soft body parts); *Fabaeformiscandona harmsworthi*: (5) female LV, (6) female RV; *Fabaeformiscandona lapponica* var. *arctica*: (7) female LV, (8) female RV, (9) male LV, (10) male RV; *Bradleystrandesia reticulata*: (11) female LV, and (12) female RV.

this species as a high-arctic form also common on Spitsbergen and in other regions in the Arctic. The female and male valves presented here are very similar to *F. lapponica* var. *arctica* in size and outline. Nevertheless, it has to be mentioned that the valve surface is covered by a pitted pattern (Fig. 11, pp. 7–10), which was originally not described by Alm (1914). Males of *F. lapponica* var. *arctica* have not been previously observed in modern records (Semenova, 2003). For several ostracod species populations of both sexes are known to indicate more favourable living conditions, whereas the parthenogenetic reproduction takes place when the environmental setting of habitats changes. The identification of *F. lapponica* var. *arctica* males is doubtless due to preserved Zenker organs (typical male reproduction organ) in some specimens. Males of *F. lapponica* var. *arctica* in unit III may indicate more favourable conditions for this species than exist today for the regions where this species has been found. To verify this argument, male specimens should be observed under modern conditions.

The species *Bradleystrandesia reticulata* (Zaddach, 1844) (Fig. 11, pp. 11–12) is broadly distributed in mid-latitudes as well as in high-latitude regions and has broad tolerance to such environmental factors (Meisch, 2000). Populations of both sexes are known from northern habitats, but probably due to the rareness of *B. reticulata* valves in our record we observed only female valves. The species has been found in East Siberia (Pietrzeniuk, 1977; Semenova, 2005), and also in Greenland and in the Siberian Arctic (Alm, 1914; Wetterich et al., 2008). Fossil records of this species were obtained in European Quaternary deposits (Griffiths, 1995), but have not been found in Siberia to date.

The fossil ostracod assemblage can be interpreted as typical for shallow water conditions with moderate water temperature variations. The habitat was most likely a pond, as these organisms are typical in today's polygonal tundra landscapes. The great rarity of ostracod findings in the studied sequence contradicts the former studies of Wetterich et al. (2005) on the Bykovsky Peninsula. The occurrence and preservation of ostracod shells in syngenetic frozen deposits of ponds in low-centred ice wedge polygon systems depends on numerous hydrological, pedological, and cryological factors. Nevertheless, the high abundance of shells in even one sample confirms that freshwater ostracods could appear in such a periglacial environment.

4.7. Insect remains

The samples for insect remains analysis were mostly taken in equal volume, but contain different numbers of individuals. The poorest sample with 43 insect remains (Bkh2002 B11, 10 m a.r.l.) comes from unit I, and the richest sample with 463 insect remains comes from the upper part of the unit IVa (Bkh 2002 B04, 31.7 m a.r.l.). The fossil insect fauna is mostly represented by beetles (order Coleoptera) whose hard chitin parts allow good preservation in non-consolidated deposits (Appendix C in Supplementary data and Fig. 12). We also found some unidentified remains from other orders such as Hymenoptera, Diptera, Trichoptera, and Hemiptera, which have not been included in the species list.

The insect association in unit I (Bkh2002 B11) consists predominantly of representatives of the typical arctic tundra group and the mesic tundra group. Insects of the steppe groups as well as the shrub, meadows, and forest groups are only secondarily represented. This spectrum does not show that there are differences between insect assemblages of the lower sand units I and II, and the Ice Complex units III and IVa (Fig. 13).

Fossil insect assemblages from the Ice Complex units III and IVa show a rather consistent composition of species representative of different ecological spectra (Fig. 13). There are almost equal abundances of xerophilous groups, mostly tundra xerophilous (ks), meso-hygrophilous tundra insects (mt), and arctic insects (tt). An increase of steppe insects is evident at about 40 kyr BP (Bkh2002 B10), but later the species composition returns to the previous one.

In the Ice Complex units III and IVa (Fig. 13) insect remains are present at an unusually high level for an arctic group, with an average of 20–30% and a maximum of up to 86% of all remains. Insects of typical and arctic tundra (tt) are represented here mostly by the willows weevil *Isochnus arcticus*. The steppe group (ss) which normally plays an important role in most late Pleistocene entomofauna records from Northeast Siberia (Kiselyov, 1981; Sher and Kuzmina, 2007) is not very abundant in the section, except for one single assemblage. Nevertheless, the character of the late Pleistocene insect fauna from Kurungnakh Island is evidently steppe–tundra. The assemblage includes such typical Pleistocene steppe–tundra species as the pill beetle *Morychus viridis*, the leaf beetles *Chrysolina brunnicornis* and *Ch. arctica*, the weevils *Coniocleonus cinerascens*, *Coniocleonus astragali*, *Coniocleonus ferrugineus*, and *Stephanocleonus fossulatus* in association with some xerophilous species, which were widespread in the Pleistocene steppe–tundra landscape and have

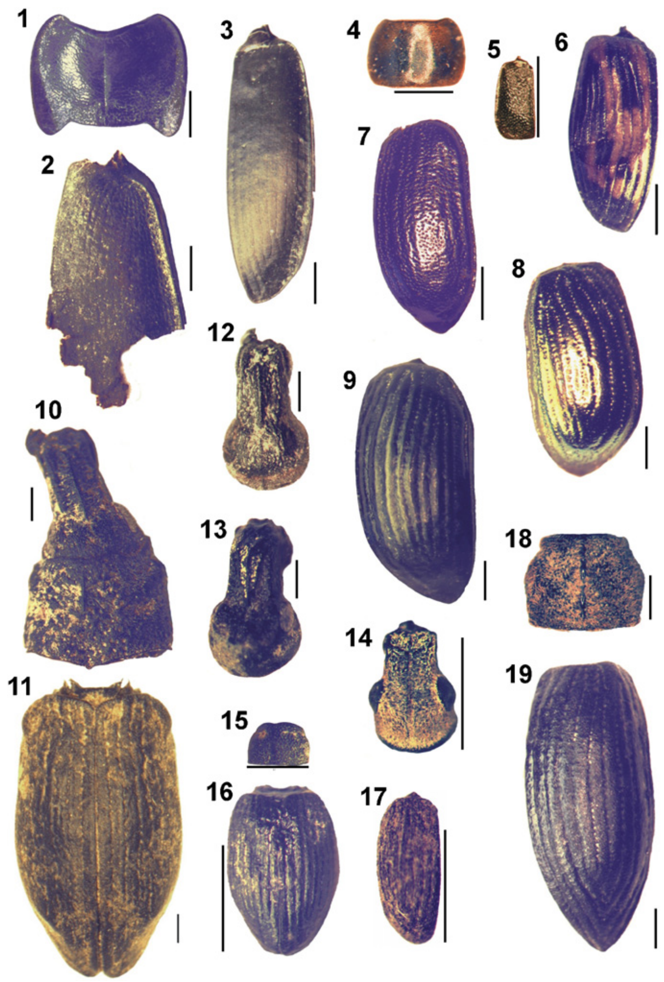

Fig. 12. Fossil insect remains from Kurungnakh Island: (1) Ground beetle *Carabus kolymensis*, pronotum; (2) Ground beetle *Carabus kolymensis*, elytron; (3) Ground beetle *Pterostichus tundrae*, elytron; (4) Rove beetle *Tachinus brevipennis*, pronotum; (5) Rove beetle *Eucnecosum* cf. *tenue*, elytron; (6) Dung beetle *Aphodius* sp., elytron; (7) Leaf beetle *Chrysomela blaisdelli*, elytron; (8) Leaf beetle *Chrysolina brunnicornis wrangeliana*, elytron; (9) Leaf beetle *Chrysolina subsulcata*, elytron; (10) Weevil *Coniocleonus cinerascens*, head and pronotum; (11) Weevil *Coniocleonus* sp., connected elytrons; (12) Weevil *Coniocleonus astragali*, head; (13) Weevil *Stephanocleonus fossulatus*, head; (14) Weevil *Sitona borealis*, head; (15) Weevil *Isochnus arcticus*, pronotum; (16) Weevil *Isochnus arcticus*, connected elytrons; (17) Weevil *Isochnus flagellum*, elytron; (18) Weevil *Lepyrus nordenskioeldi*, pronotum; and (19) Weevil *Lepyrus nordenskioeldi*, elytron. Note varying scales which correspond to 1 mm length each.

become relatively rare recently, as well as the weevils *Mesotrichapion wrangelianum*, *Hemitrichapion tschernovi*, *Sitona borealis*, *Hypera ornate*, and others. The most typical member of the steppe-tundra insect community, the weevil *Stephanocleonus eruditus*, was not found in the Kurungnakh assemblages, but was present in most samples of neighbouring outcrops (Kuzmina, unpublished data; Sher et al., 2005). Although this weevil is a significant local feature of this section, it seems to be not characteristic of the entire region,

In unit IVa the appearance of the insect assemblage changed at about 17 kyr BP (Bkh2002 B04). There is a distinct domination of arctic species with up to 86%, which have not been described in Siberian fossil insect records yet. Even the "coldest" insect assemblages (LGM) from Bykovsky Peninsula (Sher et al., 2005) contain less percent of arctic species. In general, the species diversity of this sample is low. This sample contains no true steppe insects, except for the quite cold-resistant meadow-steppe leaf beetle *Chrysolina arctica*, recently known only from Wrangel Island, East Siberian Sea. The overlying sample (Bkh2002 B03) at 33.3 m a.r.l. belongs to the early Holocene unit IVb and has lost the overwhelmingly arctic species assemblage, but it still contains more than 30% arctic insects.

The observed pattern seems to be similar to the well-studied Ice Complex sequence of Bykovsky Peninsula, Laptev Sea (Sher et al., 2005), where one stage in the section (ca 46–34 kyr BP) with mostly low occurrences of the steppe insect group and a remarkable number of arctic insects was also discovered. Nevertheless, some short intervals of slightly increasing steppe insects are present also. The Bykovsky Peninsula sediments, dated between 24 and 15 kyr BP, which corresponds to the coldest time of the LGM, is characterised by 20–67% of arctic insects.

Two samples (Bkh2002 B01 and B07) were studied from the Holocene unit V. An additional sample taken in 2000 from nearby thermokarst deposits (profile Bkh 4, Fig. 4 in Schirrmeister et al., 2003) was also analysed (Appendix C in Supplementary data). All Holocene insect assemblages are significantly different from those found in both the lower sand and the Ice Complex deposits. The Holocene entemofauna is dominated by species of wet tundra (mt) at up to 72%. The wet tundra group includes species such as the ground beetles *Diacheila polita*, *Pterostichus brevicornis*, *P. pinguedineus*, *P. vermiculosus*, and *P. agonus* as well as the rove beetles *Olophrum consimile* and *Tachinus brevipennis*.

The ground beetle *Pterostichus (Cryobius) brevicornis* is the most abundant beetle in the Holocene sediments. This is one of the most common beetles in modern tundra and forest-tundra regions. The rove beetle *O. consimile* was dominant in the thermokarst unit V. This is not surprising, since the rove beetles of *Olophrum* genus prefer boggy habitats, which are typical of succession stages of thermokarst depressions. There are also a number of other hygrophilous insects in all Holocene assemblages from Kurungnakh: the ground beetles *Dyschiriodes nigricornis*, *Agonum* sp., the rove beetle *Holoboreaphilus nordenskioeldi*, the leaf beetle *Hydrothassa hannoverana*, and the weevil *Tournotaris bimaculatus*. In addition, some forest species have been found: the ground beetle *Notiophilus sylvaticus*, the rove beetle *Phyllodrepa angustata*, and the bark beetle *Polygraphus* sp. The species diversity of shrub insects in the Holocene unit V is higher than in the Pleistocene insect assemblages. The shrub group (sh) includes the leaf beetles *Chrysomela blaisdelli* and *Phratora vulgatissima* and the weevils *Dorytomus imbecillus*, *D. rufulus amplipennis*, and *Lepyrus nordenskjoeldi*.

According to the insect studies we can discern three stages of the developing environment. During the first stage (>50–32 kyr BP), there existed a cold variant of steppe–tundra that comprises the formation of the lower sand units I and II as well as the Ice Complex unit III. The second stage (about 17 kyr BP) was characterised by dry and cold tundra conditions (unit IVa). During the Holocene (<8 kyr BP) an open tundra-like landscape occurred, probably with weakly developed forest vegetation (units IVb and V).

4.8. Mammal remains

The mammal bone collection consists of 118 bones sampled by different scientists in 2000–2002, 2005, and 2007 on the outcrops of Kurungnakh Island. Palaeontological findings from the island are also stored in the Museum of the Lena Delta Reservation, Tiksi, Russia.

According to the finding's location the bones were divided into four groups. Group A comprises eight strictly in situ-found bones, probably of one individual horse (*Equus caballus*) from the Ice Complex deposits. Additionally, another in situ horse bone was

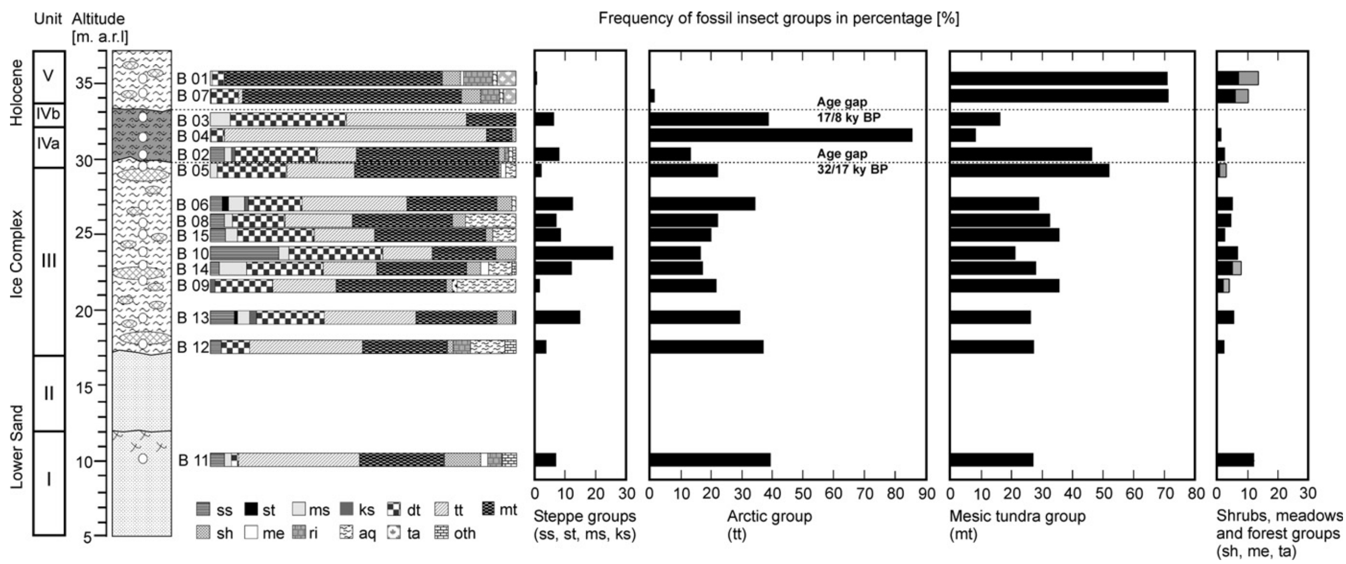

Fig. 13. Distribution of the fossil insect groups from Kurungnakh Island: (ss) insects of hemicryophytic steppe; (st) insects of thermophilic steppe; (ms) insects of meadow-steppe and steppe-like habitats in the tundra zone; (ks) xerophilic insects of different habitats; (dt) insects of dry tundra habitats; (tt) insects from typical and arctic tundra; (mt) insects of mesic tundra habitats; (sh) insects associated with shrubs; (me) insects living in meadows, mostly in the forest zone; (ri) riparian insects; (aq) aquatic insects; (ta) dendrophagous and insects restricted to the taiga zone; and (oth) other insects.

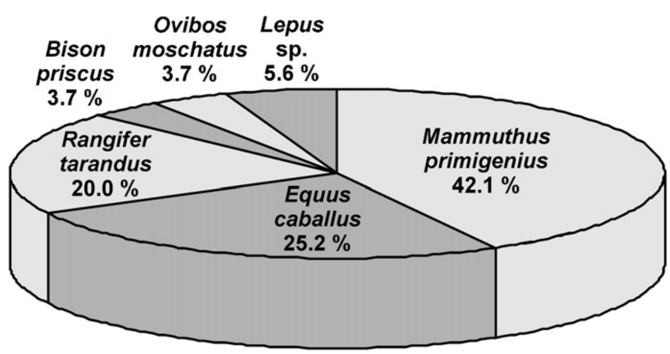

Fig. 14. Taxonomic composition of mammal bones collected from Kurungnakh Island (total number — 107 samples).

found with copulas and marrow in a state of excellent preservation. The second group B includes 37 samples from thermo-erosional cirques. Knowing the altitude of these findings (i.e. the minimum level of their original position), we can define the approximate altitude from which these bones come. Therefore, both groups A and B have direct importance for the geological interpretation of the deposits. A third group C of mammal remains were collected within the debris of the exposure. They also belong to the section. Group D includes the biggest part of the collection from Kurungnakh Island, which comes from the shore and sandbank. Such bones were probably relocated from distant outcrops by river current or ice flow. Nevertheless, such findings also reflect the association of large fossil mammals.

The composition of the studied bone collection is typical for the late Pleistocene "Mammoth Fauna" of the Siberian Arctic. Fossil remains of woolly mammoths (*Mammuthus primigenius* Blumenbach, 1799), horses (*E. caballus* Linnaeus, 1758), reindeer (*Rangifer tarandus* Linnaeus, 1758), bison (*Bison priscus* Bojanus, 1827), muskox (*Ovibos moschatus* Zimmermann, 1780), and hares (*Lepus* sp.) are found (Fig. 14). The lower horizon of the Ice Complex (unit III) contains rather abundant bone material. The bones that were found there belonged to separate individuals, e.g. several ribs and leg bones from two mammoth individuals, as well as several leg bones from one horse individual.

The taxonomical study was completed by radiocarbon dates obtained from bone collagen. In unit III several horse bones were found in situ. Large hind leg bones from one horse individual were collected from the frozen silt sediments between two peat layers at a height near 20 m a.r.l. From the same level a foreleg bone from a horse was collected and radiocarbon dated at 34 200 ± 500 yr BP (GIN 110883, BKh–O65, Schirrmeister et al., 2003). Another radiocarbon date on bone material of 31 220 ± 180 yr BP (OxA-13675, BKh–O42) also indicates the age of the Ice Complex deposits.

Palaeontological material from the thermo-erosional cirques of Kurungnakh Island is characterised by good preservation and completeness. Often different parts of a skeleton lay not far from each other. Of particular interest is the find of a woolly mammoth skeleton fragments (23 bones: vertebrae, ribs, foreleg, and hind leg bones) from the highest layers of the Ice Complex at 32–35 m a.r.l.

The species diversity of the Kurungnakh collection agrees with other records from Arctic Siberia (e.g. Kuznetsova et al., 2003; Sher et al., 2005). The large number of bones from grazing mammals mostly originating from deposits of the Kargin interstadial period (unit III) is evidence for the high bioproductivity of the tundra–steppe (mammoth steppe) vegetation during this period. This conclusion is also supported by large amounts of spores from dung-inhabiting Sordariales fungi, which were determined by palynological studies.

5. Discussion

5.1. Local stratigraphic and palaeoenvironmental interpretation

The multidisciplinary palaeo-proxy dataset allows several stages of the late Quaternary history of the study area to be distinguished (Table 5).

The lower sand formation of the section (units I and II) accumulated under changing shallow water conditions probably in a meandering fluvial milieu of the Palaeo-Lena River between 100 and 50 kyr before. This is evident by IR-OSL dating (Schwamborn et al., 2002), ^{230}Th/U dates, and a lot of indefinite

Table 5
Summary of stratigraphy, facies, and palaeecology deduced from multiproxy records

Stratigraphy	Age (kyr BP)	Palaeoenvironment						
		Sediment	Ice	Pollen	Seeds	Ostracods	Insects	Mammals
Middle/Late Holocene	6–3	*Unit V* Modern landscape of the 3rd Lena terrace	Small syngenetic ice wedges, warmer winter temperature	*PZ 5* Modern vegetation and climate conditions	Wet tundra with willow shrubs		Wet shrub tundra	
Early Holocene	≈8	*Unit IVb* Thermokarst	Small syngenetic ice wedges, warmer winter temperature	*PZ 4* Shrub tundra, climate optimum	Dry tundra or tundra steppe, no climate change recorded		Open shrub tundra	
Hiatus	17–8	No records						
Late Weichselian (Sartan) stadial	≈17	*Unit IVa* Ice complex	Huge syngenetic ice wedges, cold winter temperature	*PZ 3* Scarce arctic tundra steppe, cold and dry	Dry tundra or tundra steppe, cold and dry		Arctic tundra, cold and dry	
Hiatus	32–17	No records						
Middle Weichselian (Kargin) interstadial	50–32	*Unit III* Pediment plain in front of the Chekanovsky Ridge, Ice complex	Huge syngenetic ice wedges, cold winter temperature	*PZ 2* Arctic tundra steppe, climate optimum *PZ 1* Arctic tundra steppe, climate	Tundra steppe, generally dry, wet habitats existing	Shallow ponds with moderate temperature variations	Arctic tundra steppe, cold and dry	Optimum of the "Mammoth Fauna"
Early Weichselian (Zyryan) stadial	100–50	*Units I–II* Meandering river branch	No syngenetic ice wedges due to unstable conditions		Sparse data. Arctic tundra-steppe, cold and dry		Arctic tundra steppe, cold and dry	

radiocarbon ages >50 kyr BP (Schirrmeister et al., 2003). According to our new data, which coincide with previous datings of these widely exposed sands in the western Lena Delta, an early Weichselian (Zyryan) stadial river landscape existed there. Changing transport and accumulation conditions can be deduced from the sedimentological data from units I and II. While in unit I, small-scale interbedding, poor sorting, and repeated peat layer accumulation reflect frequently varying water runoff in a quiet, shallow river branch or near-shore area, unit II is distinguished by fine lamination, less organic material, more continuous grain sizes, and a higher degree of sorting. Such properties give evidence for stable fluvial current conditions. Probably because of meandering the course of the river branch shifted between the sedimentation of units I and II. These sediments were epigenetically frozen after their accumulation. The fluvial sedimentation conditions were unfavourable for the deposition and preservation of pollen, plant macro-fossils, insect remains, and ostracod shells in units I and II. The concentration of these fossils is therefore too low for detailed environmental interpretations. The bioindicators merely reflect the existence of a tundra–steppe environment during the time of deposition, which correspond to previous regional multiproxy records (Schirrmeister et al., 2002a–c, 2003; Sher et al., 2005).

Great change in all environmental conditions is evident with the beginning of the Middle Weichselian (Kargin) interstadial in connection with the formation of the Ice Complex unit III. Large syngenetic ice wedges, ice-supersaturated deposits, segregated ice veins, and thick cryoturbated peaty palaeosol horizons, which are characteristic for the late Pleistocene Yedoma Suite reflect the different landscape that existed between 50 and 32 kyr BP. Subaerial accumulation within a polygonal ice wedge net, which formed on a badly-drained plain in front of the Chekanovsky Ridge, is assumed for this period, with an estimated mean accumulation rate of about 12.5 cm per 100 years. In addition, decreasing values of magnetic susceptibility reveal a change of the sediment source. According to heavy mineral analysis the sediments source was the neighbouring Chekanovsky Ridge (Schwamborn et al., 2002; Schirrmeister et al., 2003). The formation of large syngenetic ice wedges clearly indicates long-term stable landscape conditions during this interval. We doubt interpretations of the Yedoma Suite as pure Arctic loess and the primarily aeolian origin (Tomirdiaro, 1982) because of poorly sorting, multimodal grain-size distribution, ice-supersaturated cryolithology, and local sediment sources (Schirrmeister et al., 2008).

Palynological spectra from unit III reflect relatively warm summer conditions for the earlier part of the Kargin interstadial about 42 kyr BP (PZ 1) and climate amelioration during the Kargin climate optimum between 40 and 32 kyr BP (PZ 2). Abundant *Pediastrum* and *Botryococcus* colonies indicate the presence of small ponds in the surrounding area and wet places may have existed in the floodplain itself during that time as is indicated by the presence of *Carex* sect. *Phacocystis* macro-fossils during most of the period. The variation of dominating insect groups is probably indicative of short-term environmental fluctuations during the entire interstadial period.

An age gap of 15 kyr between 32 kyr (units III) and 17 kyr BP (unit IVa) spans long periods of the Sartan glacial. This gap could be explained by local erosion most of the Sartan deposits. A rather similar gap between 28.5 and 12 kyr BP was recorded from Bol'shoy Lyakhovsky Island (73°N, 141°E), eastern Laptev Sea (Andreev et al., in press). Nevertheless, in other Ice Complex sequences e.g. from Bykovsky Peninsula southeast of the Lena Delta (Andreev et al., 2002; Schirrmeister et al., 2002a–c) and at Cape Mamontov Klyk (73°N, 117°E), western Laptev Sea (Schirrmeister et al., in press) complete Sartan sequences were proven. Unit IV, which is sedimentologically and cryolithologically uniform, consists of the late Sartan part (unit IVa) and the Holocene part (unit IVb). This subdivision in a scarce tundra environment (PZ 3) and more moderate shrubby tundra (PZ 4) is also clearly evident according to pollen and insect data. Therefore, unit IV probably could be considered as deposits that buried an erosional surface of the Ice Complex sequence, where late Sartan deposits were preserved between small Holocene thermokarst depressions. Layers of poorly sorted sand with low organic content indicate occasionally stronger transport energy due to sporadic surface runoff events during the late Sartan and the partial reworking of unit IVa deposits during the early Holocene. The age hiatus of almost 10 kyr between units IVa and IVb was probably caused by Holocene thermokarst processes. Nevertheless, a polygonal ice wedge system persisted for the entire time as is indicated by the continuous growth of large syngenetic ice wedges. Pollen and plant macro-remains indicate that a tundra–steppe, typical for extremely continental arctic climate, persisted during the late Sartan (unit IVa) period even though this ecosystem was probably much scarcer than before due to a temperature drop. The fossil insect records also point to very cold conditions before termination of the last glacial period.

Large changes in nearly all sedimentological parameters and palaeoecological records are evident for the uppermost middle to late Holocene part (unit V) of the sequence, which discordantly covers the frozen deposits below. This part of the sequence was accumulated from the middle Holocene on. Modern environmental conditions appeared after 5 kyr BP. Warmer winter temperatures during the late Holocene in comparison to the Kargin interstadial are deduced from the stable isotope signature of the ice wedges. The size of the polygonal ice wedge systems decreased because of warmer winter conditions as well as the newly formed small-scale thermokarst relief. All bioindicators reflect a sharp shift of environmental conditions in the Holocene. Paludification and a complete disappearance of dry habitats are the most sustained effects, indicated by plant and insect remains. The pollen record indicates a rapid warming during the early Holocene and successive cooling towards modern climate conditions in the course of the Holocene.

5.2. Beringian palaeoenvironmental context

The local records that are presented from Kurungnakh Island in the southern Lena Delta are additional pieces required to reconstruct the puzzle that is the Late Pleistocene environment and the climate dynamics of Western Beringia.

The lower sand horizon was part of a meandering fluvial system that ran parallel to the Chekanovsky Ridge. Early Weichselian fluvial deposits are widely distributed in the Laptev Sea region. Similar horizons of fluvial sands below Ice Complex deposits were also observed on Cape Mamontov Klyk in front of the Pronchishchev Ridge at the western Laptev Sea coast (Schirrmeister, 2004; Schirrmeister et al., in press) and on the Bykovsky Peninsula in front of the Kharaulakh Ridge southeast of the study site (Schirrmeister et al., 2002a). The formation of such deposits was explained by Galabala (1987) as accumulation of a huge alluvial fan of the Lena River within a closed non-marine basin. This interpretation is similar to our opinion. According to Schwamborn et al. (2002) and Schirrmeister et al. (2003) the sandy units were formed on a flood plain of the Early Weichselian Lena River and intensified fluvial activities are assumed for the Early Weichselian (Zyryan) period. The landscape-forming processes in the study region probably pertained to a more comprehensive reorganisation of the hydrological systems in northern Eurasia. For example, Mangerud et al. (2004) have reported on the rerouting of the drainage in northern Eurasia during this period connected with changing orientation of glacial meltwater runoff.

The Ice Complex horizon on Kurungnakh Island belongs to the Yedoma Suite of the Northeast Siberian Quaternary stratigraphy (Sher et al., 1987). The studied horizon contains primarily middle Weichselian (Kargin) interstadial records and a part of Late Weichselian (Sartan) stadial. Sedimentological, cryolithological, pollen, plant macro-fossil, and insect data sets are similar to those of the Kargin sequence on Bykovsky Peninsula (Andreev et al., 2002; Kienast et al., 2005; Sher et al., 2005). For most of the sedimentation time (>50 to about 32 kyr BP), the palaeoecological records from Kurungnakh Island indicate the existence of tundra–steppe vegetation under a cold continental climate. In contrast to the Ice Complex sequence on the Bykovsky Peninsula (Andreev et al., 2002; Kienast et al., 2005; Sher et al., 2005), the Kargin interstadial climate was possibly somewhat cooler during the summer periods. The Bykovsky Peninsula was most likely climatically favoured by the proximity of the Kharaulakh Mountain range, which hampered cloud formation, trapped rainfall coming from the west, and caused warm southerly winds (foehn). According to Arkhipov et al. (2005) the Kargin interstadial in West Siberia lasted from 55–50 to 23 kyr BP and consisted of three warming periods separated by two cooling periods (44–42 and 35–30 kyr BP). In Central Yakutia the duration of the Kargin period is given between 42–43 and 25–26 kyr BP (Fradkina et al., 2005a). In the Yana-Indigirka lowland the Kargin interstadial between 50 and 26 kyr BP was also characterised by three warming and two cooling phases (Fradkina et al., 2005b). The younger Kargin sediments were not preserved in the studied sequence. Therefore, our palaeoecological records reflect at least some weak environmental fluctuations during approximately 42–32 kyr BP, which probably correspond to the end of the first cooling and the next warming period. Interstadial records were evident also in the eastern region of the Beringian landmass during the Kargin period. In Alaska the Middle Wisconsin was also characterised by stronger soil formation and accumulation of detritic organic beds (Hopkins, 1982) as well as downward thawing of permafrost and ice wedges in the Fairbanks area about >38 kyr BP, which was connected with a warmer period during the Middle Wisconsin time (Péwé, 1975). In addition, Berger (2003) refers several papers about a MIS warming between 40 and 30 kyr BP in northwest and Central Alaska as well as in the Canadian Yukon Territory. Finally, Anderson and Lozhkin (2001) summarise most of the Beringian MIS 3 records available ten years before. Between 30–26 and 39–33 kyr BP the climate was as warm or nearly as warm as present whereas cool and dry intervals occurred between 33–30 and 45–39 kyr BP. That also corresponds with our local interpretation from Kurungnakh Island of climate variations during the studied MIS3 time frame.

The sharp cut of the sequence at about 32 kyr BP and the absence of about 15 kyr of sedimentation are probably connected with strong erosional processes due to neotectonic seismic events on the seismically highly active rift region at the northeastern border of the Eurasian continental plate (Drachev et al., 1998; Franke et al., 2000). Similar explanations are given for the lack of the Sartan stage in Ice Complex deposits on Bol'shoy Lyakhovsky Island (Andreev et al., in press).

The degradation of permafrost by thermokarst processes and the transgression of the arctic shelf seas due to global warming were the most radical environmental impacts on the entire arctic and subarctic Siberian lowlands during the late Pleistocene–Holocene transition period. Ice-rich permafrost sequences in Siberia are therefore often not complete on the top because of thermokarst processes and discontinued accumulation. A strong reorganisation of hydrological systems and the entire periglacial landscape is evident during this highly dynamic transition period (e.g. Grosse et al., 2007).

The Holocene climate optimum in Arctic Siberia was characterised by the spreading of warmth-loving species associations, especially of shrubby tundra and trees. This is also reported by some other studies in the Siberian Arctic.

6. Conclusions

The sedimentation regimes in the periglacial palaeo-landscapes changed repeatedly during the late Quaternary (meandering fluvial, proluvial or colluvial, and thermokarst-affected). Erosional events occurred as a consequence of permafrost degradation and likely neotectonic seismic activity.

The studied sequence covers a time of various glacial/interglacial and stadial/interstadial climate variations. The corresponding stratigraphic configuration of the Late Pleistocene to Holocene sequence on Kurungnakh Island correlates well with the regional stratigraphy in northeastern Siberia and with Eurasian equivalents (Early, Middle, and Late Weichselian, Holocene) as well as global analogues (MIS 4–1).

Between >50 and 32 kyr BP, the palaeoecological records indicate the existence of tundra–steppe vegetation under a cold continental climate. After a sedimentation gap at the termination of the Late Weichselian cold stage, extremely cold-arid conditions prevailed in the study area according to bioindicators. At the beginning of the Holocene, the tundra–steppe disappeared completely due to lasting paludification. A shrub tundra formed with boreal elements like *A. fruticosa*, which later retreated in response to the late Holocene cooling.

Acknowledgements

The studies presented were part of the Russian–German cooperative scientific effort, "System Laptev Sea". Studies of pollen and plant macro-fossils as well as geochronology were funded by the German Science Foundation (DFG) within the framework of three different projects (SCHI 975/1 late Quaternary warm phases in the Arctic; KI 849/1 Environmental history of Northern Siberia; FR 877/15-1, Interstadial and interglacial periods). During recent years the Russian-German cooperation was also promoted by several guest science supports from DFG and DAAD (German Academic Exchange Service). We thank all colleagues who helped us during fieldwork (e.g. sampling of bones by Marina V. Dorozkina, Elena Y. Pavlova, Waldemar Schneider) as well as during the analytical work in the laboratories at the Alfred Wegener Institute Potsdam (Ute Bastian, Antje Eulenburg, Lutz Schönicke) and at the GGA-Institute Hannover (Sabine Mogwitz). We thank the Otto Schmidt Laboratory (St. Petersburg, Russia) for the opportunity to use photo equipment for the insect illustrations and Helga Kemnitz (GeoForschungsZentrum Potsdam, Germany) for help in SEM photography of ostracod valves. The paper benefited by English language correction and valuable comments from Candace O'Connor (UAF, Fairbanks, Alaska) as well as by highly constructive suggestions from two anonymous reviewers.

Appendix. Supplementary data

Supplementary data associated with this article can be found in the online version at doi:10.1016/j.quascirev.2008.04.007.

References

Alm, G., 1914. Beiträge zur Kenntnis der nördlichen und arktischen Ostracodenfauna (contributions to the knowledge of Nordic and Arctic ostracods). Arkiv för Zoologi (Archive for Zoology) 9, 1–20 (in German).

Anderson, P.M., Lozhkin, A.V., 2001. The stage 3 interstadial complex (Karginskii/middle Wisconsinan interval) of Beringia: variations in paleoenvironments and implications for paleoclimatic interpretations. Quaternary Science Reviews 20, 93–125.

Andreev, A.A., Schirrmeister, L., Siegert, C., Bobrov, A.A., Demske, D., Seiffert, M., Hubberten, H.-W., 2002. Paleoenvironmental changes in north-eastern Siberia during the Late Pleistocene—evidence from pollen records of the Bykovsky Peninsula. Polarforschung 70, 13–25.

Andreev, A., Grosse, G., Schirrmeister, L., Kuznetsova, T.V., Kuzmina, S.A., Bobrov, A.A., Tarasov, P.E., Novenko, E.Yu., Meyer, H., Derevyagin, A.Yu., Kienast, F., Bryantseva, A., Kunitsky, V.V., Weichselian and Holocene palaeoenvironmental history of the Bol'shoy Lyakhovsky Island, New Siberian Archipelago, Arctic Siberia. Boreas, in press.

Arkhipov, S.A., Volkova, V.S., Zolkina, V.S., Krutkover, A.A., Kul'kova, L.A., 2005. West Siberia. In: Velichko, A.A., Nechaev, V.P. (Eds.), Cenozoic Climatic and Environmental Changes in Russia. The Geological Society of America Special Paper 182, pp. 105–120.

Astakhov, V., 2001. The stratigraphic framework for the Upper Pleistocene of the glaciated Russian Arctic: changing paradigms. Global and Planetary Change 31, 283–295.

Astakhov, V., 2006. Chronostratigraphic subdivisions of the Siberian Upper Pleistocene. Russian Geology and Geophysics 47, 1207–1220.

Astakhov, V., Mangerud, J., 2005. The age of the Karginsky interglacial strata on the lower Yenisei. Doklady Earth Sciences 403, 673–676.

Berger, G.W., 2003. Luminescence chronology of late Pleistocene loess paleosol and tephra sequences near Fairbanks, Alaska. Quaternary Research 60, 70–83.

Bobrov, A.A., Andreev, A.A., Schirrmeister, L., Siegert, C., 2004. Testate amoebae (Protozoa: Testacea) as bioindicators in the Late Quaternary deposits of the Bykovsky Peninsula, Laptev Sea, Russia. Palaeogeography Palaeoclimatology Palaeoecology 209, 165–181.

Craig, H., 1961. Isotopic variations in meteoric waters. Science 133, 1702–1703.

Drachev, S.S., Savostin, L.A., Groshev, V.G., Bruni, I.E., 1998. Structure and geology of the continental shelf on the Laptev Sea, Eastern Russian Arctic. Tectonophysics 298, 357–393.

Fradkina, A.F., Alekseev, M.N., Andreev, A.A., Klimanov, V.A., 2005a. East Siberia. In: Velichko, A.A., Nechaev, V.P. (Eds.), Cenozoic climatic and environmental changes in Russia. The Geological Society of America Special Paper 382, pp. 89–103.

Fradkina, A.F., Grinenko, O.V., Laukhin, S.A., Nechaev, V.P., Andreev, A.A., Klimanov, V.A., 2005b. North-eastern Asia. In: Velichko, A.A., Nechaev, V.P. (Eds.), Cenozoic Climatic and Environmental Changes in Russia. The Geological Society of America Special Paper 382, pp. 105–120.

Franke, D., Hinz, K., Block, M., Drachev, S.S., Neben, S., Kos'ko, M.K., Reichert, C., Roeser, H.A., 2000. Tectonics of the Laptev Sea Region in Northeastern Siberia. Polarforschung 68, 51–58.

Frechen, M., Sierralta, M., Oezen, D., Urban, B., 2007. Uranium-series dating of peat from Central and Northern Europe. In: Sirocko, F., Litt, T., Claussen, M. (Eds.), The Climate of Past Interglacials. Springer, Heidelberg, pp. 92–118.

Fry, B., Brand, W., Mersch, F.J., Tholke, K., Garrit, R., 1992. Automated analysis system for coupled ^{13}C and ^{15}N measurements. Analytical Chemistry 64, 288–291.

Galabala, R.O., 1987. Novye dannye o stroenii del'ty Leny (New data on the Lena Delta structure). In: Pokhilainen, V.P. (Ed.), Chetvertichniy Period v Severno-Vostochoy Azii (Quaternary of North East Asia). SVKNII DVO AN SSSR, Magadan, pp. 152–172 (in Russian).

Griffiths, H.I., 1995. European Quaternary Freshwater Ostracoda: a biostratigraphic and Paleobiogeographic primer. Scopolia 34, 168pp.

Grigoriev, M.N., 1993. Kriomorfogenez ust'evoi oblasti reki Leny (Cryomorphogenesis of the Lena River mouth). RAS SB Publishers, Permafrost Institute Yakutsk (in Russian).

Grigoriev, M.N., Rachold, V., Bolshiyanov, D.Y., Pfeiffer, E.-M., Schirrmeister, L., Wagner, D., Hubberten, H.-W. (Eds.), 2003. Russian-German Cooperation SYSTEM LAPTEV SEA: the Expedition LENA 2002, Reports on Polar and Marine Research, 466, 341 pp.

Grimm, E., 1991. TILIA and TILIAGRAPH. Illinois State Museum, Springfield, IL, USA.

Grosse, G., Schirrmeister, L., Siegert, C., Kunitsky, V., Slagoda, E.A., Andreev, A.A., Dereviagyn, A.Y., 2007. Geological and geomorphological evolution of a sedimentary periglacial landscape in Northeast Siberia during the Late Quaternary. Geomorphology 86, 25–51.

Hopkins, D.M., 1982. Aspects of the paleogeography of Beringia during the Late Pleistocene. In: Hopkins, D.M., Matthews, Jr., J.V., Schwerger, C.E., Young, S.B. (Eds.), Paleoecology of Beringia. Academy Press, NY, London, pp. 3–27.

Hubberten, H.-W., Andreev, A., Astakhov, V.I., Demidov, I., Dowdeswell, J.A., Henriksen, M., Hjort, C., Houmark-Nielsen, M., Jakobsson, M., Kuzmina, S., Larsen, E., Lunkka, J.P., Lyså, A., Mangerud, J., Möller, P., Saarnisto, M., Schirrmeister, L., Sher, A.V., Siegert, C., Siegert, M.J., Svendsen, J.I., 2004. The periglacial climate and environment in northern Eurasia during the Last Glaciation. Quaternary Science Reviews 23, 1333–1357.

Ilyashuk, B.P., Andreev, A.A., Bobrov, A.A., Tumskoy, V.E., Ilyashuk, E.A., 2006. Interglacial history of a palaeo-lake and regional environment: a multi-proxy study of a permafrost deposit from Bol'shoi Lyakhovsky Island, Arctic Siberia. Journal of Paleolimnology 36, 855–872.

Kienast, F., Schirrmeister, L., Siegert, S., Tarasov, P., 2005. Palaeobotanical evidence for warm summers in the East Siberian Arctic during the last cold stage. Quaternary Research 63, 283–300.

Kienast, F., Tarasov, P., Schirrmeister, L., Grosse, G., Andreev, A.A., 2008. Continental climate in the East Siberian Arctic during the last interglacial: implications from palaeobotanical records. Global and Planetary Change 60, 535–562.
Kind, N.V., 1974. Geokhronologia pozdnego Antropogena po izotopnym dannym (Geochronology of the late Anthropogene based on isotope data). Nauka, Moscow (in Russian).
Kiselyov, S.V., 1981. Pozdnekainozoiskie zhestkokrylie Severo-Vostoka Sibiri (Late Cenozoic Coleoptera of North-East Siberia). Nauka, Moscow (in Russian).
Krbetschek, M.R., Gonser, G., Schwamborn, G., 2002. Luminescence dating results on sediment sequences of the Lena Delta. Polarforschung 70, 83–88.
Kunitsky, V.V., 1989. Kriolitologiya nizov'ya Leny (Cryolithogenesis of the Lower Lena). RAS SB Publishers, Permafrost Institute Yakutsk (in Russian).
Kuzmina, S., Sher, A., 2006. Some features of the Holocene insect faunas of northeastern Siberia. Quaternary Science Reviews 25, 1790–1820.
Kuznetsova, T.V., Sulerzhitsky, L.D., Andreev, A., Siegert, C., Schirrmeister, L., Hubberten, H.-W., 2003. Influence of Late Quaternary paleoenvironmental conditions on the distribution of mammals in the Laptev Sea Region. In: Storer, J.E. (Ed.), Third International Mammoth Conference Yukon, Canada, Program and Abstracts. Occasional Papers in Earth Sciences, vol. 5, pp. 58–60.
Lungersgauzen, G.F., 1961. Geological History of the middle Lena and Some Questions of Quaternary Deposits Stratigraphy in East Siberia. Materialy vsesoyusnogo soveshchaniya po izucheniyu chetvertichnogo perioda tom 3. (Contributions to the All-Union Conference on the Study of the Quaternary period), vol. 3. SAS Publishers, Moscow, pp. 209–217 (in Russian).
Mangerud, J.M., Jacobsson, M., Alexanderson, H., Astakhov, V., 2004. Ice-dammed lakes and rerouting of the drainage of northern Eurasia during the Late Glaciation. Quaternary Science Reviews 23, 1313–1332.
Meisch, C., 2000. Freshwater Ostracoda of Western and Central Europe. Spektrum, Heidelberg.
Meyer, H., Schönicke, L., Wand, U., Hubberten, H.-W., Friedrichsen, H., 2000. Isotope studies of hydrogen and oxygen in ground ice—experiences with the equilibration technique. Isotopes in Environmental and Health Studies 36, 133–149.
Meyer, H., Siegert, C., Dereviagin, A., Hubberten, H.-W., 2002a. Paleoclimatic studies on Bykovsky Peninsula, North Siberia—hydrogen and oxygen isotopes in ground ice. Polarforschung 70, 37–51.
Meyer, H., Dereviagin, A.Y., Siegert, C., Schirrmeister, L., Hubberten, H.-W., 2002b. Paleoclimate reconstruction on Big Lyakhovsky Island, North Siberia—hydrogen and oxygen isotopes in ice wedges. Permafrost and Periglacial Processes 13, 91–105.
Nadeau, M.J., Schleicher, M., Grootes, P.M., Erlenkeuser, H., Gottdang, A., Mous, D.J.W., Sarnthein, J.M., Willkomm, H., 1997. The Leibniz-Labor facility at the Christian-Albrecht-University, Kiel, Germany. Nuclear Instruments and Methods in Physics Research 123, 22–30.
Nadeau, M.J., Grootes, P.M., Schleicher, M., Hasselberg, P., Rieck, A., Bitterling, M., 1998. Sample throughput and data quality at the Leibniz-Labor AMS facility. Radiocarbon 40, 239–245.
Neale, J.W., 1969. The Freshwater Ostracode Candona harmsworthi SCOTT from Franz Josef Land and Novaya Zemlya. In: Neale, J.W. (Ed.), The Taxonomy, Morphology and Ecology of Recent Ostracoda. Oliver and Boyd, Edinburgh, pp. 222–236.
Péwé, T.L., 1975. Quaternary Geology of Alaska. Geological Survey Professional Paper 835. US Government Printing Office, Washington, DC, 145pp.
Pietrzeniuk, E., 1977. Ostracoden aus Thermokarstseen und Altwässern in Zentral-Jakutien (Ostracods from thermokarst lakes and old branches in Central Yakutia). Mitteilungen des Zoologischen Museums zu Berlin (Reports of the Zoological Museum Berlin) 53, 331–362 (in German).
Pitulko, V.V., Nikolsky, P.A., Girya, E.Yu., Basilyan, A.E., Tumskoy, V.E., Koulakov, S.A., Astakhov, S.N., Pavlova, E.Yu., Anisimov, M.A., 2004. The Yana RHS site: humans in the Arctic before the Last Glacial Maximum. Science 303, 52–56.
Rachold, V. (Ed.), 1999. Expeditions in Siberia in 1998. Reports on Polar and Marine Research, 315, 268pp.
Rachold, V., Grigoriev, M.N. (Eds.), 2001. Russian-German Cooperation System Laptev Sea 2000: The Expedition LENA 2000. Reports on Polar and Marine Research, 388, 135pp.
Schirrmeister, L. (Ed.), 2004. Expeditions in Siberia in 2003. Reports on Polar and Marine Research, 489, 231pp.
Schirrmeister, L., Kunitsky, V., Grosse, G., Kuznetsova, T., Kuzmina, S., Bolshiyanov, D., 2001. Late Quaternary and recent environmental situation around the Olenyok Channel (western Lena Delta) and on Bykovsky Peninsula. Reports on Polar and Marine Research 388, 85–135.
Schirrmeister, L., Siegert, C., Kunitsky, V.V., Grootes, P.M., Erlenkeuser, H., 2002a. Late Quaternary ice-rich Permafrost sequences as a paleoenvironmental archive for the Laptev Sea Region in northern Siberia. International Journal of Earth Sciences 91, 154–167.
Schirrmeister, L., Siegert, C., Kuznetsova, T., Kuzmina, S., Andreev, A.A., Kienast, F., Meyer, H., Bobrov, A.A., 2002b. Paleoenvironmental and paleoclimatic records from permafrost deposits in the Arctic region of Northern Siberia. Quaternary International 89, 97–118.
Schirrmeister, L., Oezen, D., Geyh, M.A., 2002c. ^{230}Th/U Dating of frozen peat, Bol'shoy Lyakhovsky Island (Northern Siberia). Quaternary Research 57, 253–258.
Schirrmeister, L., Grosse, G., Schwamborn, G., Andreev, A.A., Meyer, H., Kunitsky, V.V., Kuznetsova, T.V., Dorozhkina, M.V., Pavlova, E.Y., Bobrov, A.A., Oezen, D., 2003. Late Quaternary history of the accumulation plain north of the Chekanovsky Ridge (Lena Delta, Russia): a multidisciplinary approach. Polar Geography 27, 277–319.
Schirrmeister, L., Kunitsky, V.V., Grosse, G., Kuznetsova, T., Meyer, H., Derivyagin, A.Yu., Wetterich, S., Siegert, C., 2008. The Yedoma suite of the northeastern Siberian shelf region—characteristics and concept of formation. In: Kane, D.L., Hinkel, K.M. (Eds.), Proceedings of the Ninth International Conference on Permafrost (NICOP), June 26–July 03 2008, Fairbanks, AL, USA, in press.
Schirrmeister, L., Grosse, G., Kunitsky, V.V., Magens, M., Meyer, H., Derivyagin, A.Yu., Kuznetsova, T., Andreev, A.A., Babiy, O., Kienast, F., Grigoriev, M., Preusser, F. Periglacial landscape evolution and environmental changes of Arctic lowland areas during the Late Quaternary (Western Laptev Sea coast, Cape Mamontov Klyk). Polar Research, in press.
Schwamborn, G., Andreev, A.A., Rachold, V., Hubberten, H.-W., Grigoriev, M.N., Tumskoy, V., Pavlova, E.Yu., Dorozhkina, M.V., 2002. Late Quaternary sedimentation history of the Lena Delta. Quaternary International 89, 119–134.
Semenova, L.M., 2003. Vidovoi sostav i rasprostranenie ostrakod (Crustacea, Ostracoda) v vodoemakh arkhipelaga Novaya Zemlya i ostrova Vaigach (species occurrence and distribution of ostracods (Crustacea, Ostracoda) on Novaya Zemlya Archipelago and Vaigach Island). Biologiya Vnutrennikh Vod (Biology of Inland waters) 2, 20–26 (in Russian).
Semenova, L.M., 2005. Fauna i rasprostranenie ostracod (Crustacea, Ostracoda) vo vnytrennikh vodoemakh Rossii i sopredel'nykh gosudarstv (fauna and distribution of ostracods (Crustacea, Ostracoda) in inland waters of Russia and adjacent states). Biologiya Vnutrennikh Vod (Biology of Inland waters) 3, 17–26 (in Russian).
Sher, A., Kuzmina, S., 2007. Beetle records/Late Pleistocene of Northern Asia. In: Elias, S. (Ed.), Encyclopaedia of Quaternary Science, vol. 1. Elsevier, Amsterdam, pp. 246–267.
Sher, A.V., Kaplina, T.N., Ovander, M.G., 1987. Unifitsirovanaya regional'naya stratigraficheskaya skhema chetvertichnykh otlozhenii Yano-Kolymskoi nizmenosti i ee gornogo obramleniya (Unified regional stratigraphic chart for the Quaternary deposits in the Yana-Kolyma Lowland and its mountainous surroundings). Ob'yasnatel'naya zapiska—Resheniya mezhvedomstvogo stratigraficheskogo soveshaniya po chetvertichnoi sisteme Vostoka SSSR (Explanatory Note—Decisions of Interdepartmental Stratigraphic Commission on the Quaternary of the Eastern USSR). SAS FEB Publishers, North-Eastern Complex Research Institute Magadan, pp. 29–69 (in Russian).
Sher, A.V., Kuzmina, S.A., Kuznetsova, T.V., Sulerzhinsky, L.D., 2005. New insights into the Weichselian environment and climate of the East Siberian Arctic, derived from fossil insects, plants, and mammals. Quaternary Science Reviews 24, 533–569.
Stuiver, M., Reimer, P.J., Bard, E., Beck, J.W., Burr, G.S., Hughen, K.A., Kromer, B., McCormac, G., van der Plicht, J., Spurk, M., 1998. INTCAL98 radiocarbon age calibration, 24,000–0 cal BP. Radiocarbon 40, 1041–1083.
Tomirdiaro, S.V., 1982. Evolution of lowland landscapes in northern Asia during Late Quaternary time. In: Hopkins, D.V., Matthews, Jr., J.V., Schweger, Ch.E., Young, S.B. (Eds.), Paleoecology of Beringia. Academic Press, New York, pp. 29–37.
van Everdingen, R., (Ed.), 1998 (revised May 2005). Multi-Language Glossary of Permafrost and Related Ground-Ice Terms. National Snow and Ice Data Center/World Data Center for Glaciology, Boulder, CO. ⟨http://nsidc.org/fgdc/glossary/⟩.
Vasil'chuk, Y.K., 1992. Izotopno-kislorodnyi sostav podzemnykh l'dov—Opyt paleogeokriologicheskikh rekonstrultsii (Oxygen Isotope Composition of Ground Ice—Application to Paleogeocryological Reconstructions). Moscow State University Publishers, Moscow (in Russian).
Wetterich, S., Schirrmeister, L., Pietrzeniuk, E., 2005. Freshwater Ostracodes in Quaternary permafrost deposits in the Siberian Arctic. Journal of Paleolimnology 34, 363–374.
Wetterich, S., Schirrmeister, L., Meyer, H., Viehberg, F.A., Mackensen, A., 2008. Arctic freshwater ostracods from modern periglacial environment in the Lena River Delta (Siberian Arctic, Russia): geochemical applications for palaeoenvironmental reconstructions. Journal of Paleolimnology 39, 427–449.